SYNTHESIS AND CHARACTERIZATION OF MORINGA OLEIFERA WITH REDUCED GRAPHENE OXIDE NANOCOMPOSITE FOR ADSORPTIVE REMOVAL OF IRON FROM GROUND WATER

M.Sc. THESIS

FELEKE GUADIE

DECEMBER, 2023

WOLKITE, ETHIOPIA

Wolkite University

School of Graduate studies

Synthesis and Characterization of Moringa Olifera with Reduced Graphene Oxide Nano composite for adsorptive removal of iron from ground water

A Thesis Submitted to the School of Graduate studies, in Partial Fulfillment of the Requirements for the Degree of Master of Science in Chemistry (Analytical)

Feleke Guadie

Major Advisor: Tassew Belete (ass.prof)

Co-Advisor: Megersa Feyissa (Ph.D)

December, 2023

Wolkite, Ethiopia

Approval sheet

School of Graduate studies

Wolkite University

We hereby certify that we have read and evaluated this Thesis entitled "**Synthesis and Characterization of Moringa Olifera with Reduced Graphene Oxide Nano composite for adsorptive removal of iron from ground water**" prepared under my guidance by Feleke Guadie. We recommended that it be submitted as fulfilling the thesis requirement.

……	…….	……...
Name of Major Advisor	Signature	Date
……	…….	……...
Name of Co-advisor	Signature	Date

As a member of the Board of Examiners of MSc Thesis Open Defense Examination, we certify that we have read and evaluated the Thesis prepared by Feleke Guadie Alemu and examined the candidate. We recommended that the Thesis be accepted as fulfilling the Thesis requirements for the degree of Master of Science in chemistry (Analytical).

……	…….	……...
Name of Chairman	Signature	Date
……	……	……...
Name of Internal Examiner	Signature	Date
……	…….	……...
Name of External Examiner	Signature	Date
……	…….	……...
SGS approval	Signature	Date

Declaration

I, the undersigned, declare that this thesis, entitled **"Synthesis and Characterization of Moringa Olifera with Reduced Graphene Oxide Nano composite for adsorptive removal of iron from ground water"** is my original work under the supervision of Tassew Belete except for quotations and citations which have been fully acknowledged. I also declare that it has not been previously or currently submitted for any other degree at WKU and other institution.

Name: Feleke Guadie Alemu

Signature: _____

I hereby certify that the thesis entitled "**Synthesis and Characterization of Moringa Olifera with Reduced Graphene Oxide Nano composite for adsorptive removal of iron from ground water**" prepared by Feleke Guadie under my direction has been submitted for examination with my approval as University advisor.

_____	_____	_____
Major Advisor	Signature	Date
_____	_____	_____
Co-advisor	Signature	Date

Acknowledgment

First of all, I want to give my unshared thanks to the almighty God for His total unseen and seen involvement in this work. My deepest and most heartfelt acknowledgement goes to my advisor, Tassew Belete, Assistant Professor of Analytical Chemistry, for his total involvement and patient guidance throughout my work from its very beginning to the end. He has served as a great mentor and friend from whom I have learned plenty, and he allowed me to pursue the research and kept me on the right track. I would like to thank my co-advisor, Dr Megersa Feyissa, for his technical and moral support during my work. I also would like to express my deepest gratitude to my family, especially my spouse Minalu Getaneh, my son Natnael Feleke, my mother, brothers, and sisters, for their encouragement and moral support. I would like to express my respect, love, and appreciation to all of my friends who encouraged me to do this work, for they are the ones who shaped me to make my own decisions.

Finally, I want to give my great thanks to Endegagn Woreda water, mining, energy office and Wolkitie University for giving me a chance for my MSc program, the Chemistry Department for their support in completing my studies and Institutions including Addis Abeba University, Adama Science and Technology College, Gubrie BGI Ethiopia Beer Factory allowed instruments for analysis my result materials.

List of abbreviations

EC	Electric Conductivity
EDTA	Ethylene Diamine tetraacitic acid
EPA	Environmental Protection Agency
FT-IR	Fourier Transform Infrared Radiation
GO	Graphene Oxide
MOSP	*Moringa Oleifera* Seed Powder
pH	Potential of Hydrogen
ppm	Parts Per Million
rGO	reduced Graphene Oxide
rGO/ MO	reduced Graphene Oxide and *Moringa Olifera* composite
SEM	Scanning Electron Microscope
TH	Total Hardness
TDS	Total Dissolved Solid
UV-VIS	Ultraviolet visible spectroscopy
VDW	Vender Walls interaction
WHO	World Health Organization
XRD	X- Ray Diffraction

TABLE OF CONTENTS

List of tables page

List of figures page

Abstract

Treatment of potable ground water in rural areas is still a serious problem in Ethiopia. This study was conducted to investigate low-cost, environmental friendly and innovative composite adsorbent (rGO/MO) for the removal of elevated ferrous iron (Fe^{2+}) from three randomly selected shallow well water samples. All water samples were analyzed by different parameters like pH, temperature, electrical conductivity, turbidity, TDS, TSS, hardness, chlorides, alkalinity and Fe^{2+} Concentration. The results of the study were ranged as pH (6.52-–7.22), Temperature (21.3–22.7 ℃), E.C (76.8–151.3 µS/cm), turbidity (15–22 NTU),TDS (79.2–121.3 mg/L), TSS (50–100 mg/L), hardness(120–280 mg/L), chlorides(93–125 mg/L), alkalinity (200–550 mg/L) and Fe^{2+}(0.62–0.66 mg/L). The values of most of the parameters such as pH, conductivity, temperature, TDS, hardness, and chloride content were within the permissible limit of WHO and EEPA. However, the concentration of Fe^{2+} was above the maximum permissible limit set by WHO. Similarly, the values of physicochemical parameters such as turbidity, TSS, and alkalinity were above the acceptable range for drinking water limit set by WHO and EEPA. Thus, the result showed that the potable ground water collected from rural areas pose a risk to human health unless a proper water treatment system is implemented. The investigated adsorbents (MO, rGO, and rGO/MO) were characterized by FTIR, SEM, XRD and UV-Visible techniques. An adsorption results showed remarkable adsorption capacity (q_{max}) of 44.6 mg/g as obtained from the experiment. The adsorption efficiency of rGO/MO adsorbent for elevated ferrous iron removal was affected by parameters like initial metal concentration, contact time, pH, and adsorbent dose. The highest adsorption efficiency was observed (99.2 %) at pH 9. The optimum contact time for the adsorption process was found to be at 50 minutes. The amount of Fe^{2+} ions adsorbed decreases with increasing in initial metal ion concentration. FT-IR data indicated that the adsorption of metal ions occurs on the surface of rGO/MO powder as the main functional groups that are responsible for metal ions binding are involved in the process. The Langmuir isotherm data Fe^{2+} has good fit with the experimental data (R^2=0.994) than Freundlich isotherm data Fe^{2+} (R^2=0.979).

***Key words**: -Iron, Adsorption, Moringa Olifera, Graphene oxide, ground water.*

1. INTRODUCTION

1.1. Back ground of the study

Water has vital involvement in human daily activities and their lives are depending on it. It is fundamental for the total growth and economic development of every country. Water used for domestic, industrial, and livestock in the world [1]. Chemically, the Earth is around 71% water, but 95.6% of that water is held in the seas and is not suitable for human use. According to estimates from the World Health Organization (WHO), 1.1 billion people worldwide still lack access to treated drinking water supplies, and 2.4 billion do not have access to adequate sanitation. It should be acknowledged that having access to clean water is one of the top humanitarian priorities, but that it is still a challenge because of the population growth and accelerated anthropogenic activity that also cause pollution to be released, especially heavy metals that are specific to water bodies [2].

Ground water is usually considered as much cleaner than surface water. However, many factors like, discharge of industrial, agricultural and domestic waste water, land use practices, geological formation, rainfall patterns and infiltration rate affect the groundwater quality [3].

Over the years, one of the main causes of water contamination has been heavy metals. Because these heavy metals do not degrade into harmless forms, an imbalance between the aquatic flora and fauna develops, which in turn has an impact on human health. Stomach pains, vomiting, diarrhea, typhoid, cancer, hormonal imbalance, infertility, and severe liver and kidney damage are among the harmful consequences of heavy metals on humans [2]. Among these, iron is the second most prevalent metal in the earth and is one of the heavy metals found in water. It is the fourth element in the earth's crust and is mostly found in groundwater. In deeper wells with little to no oxygen, iron is a prevalent metallic element that naturally exists together. Weathering of minerals containing iron, such as amphibole, iron sulfide, and iron-rich clay minerals, is one of iron's natural sources. Magnetite, hematite, goethite, and siderite are the primary naturally occurring iron minerals. Weathering processes let the substance out. Iron carbonate is present in both mineral and drinking water. Iron will also dissolve in the groundwater where it passes through organically rich soil. Anthropogenic sources of iron can also include acid mine drainage, landfill leaks, and industrial effluents. Groundwater can also contain iron from well casing, pump components, pipes, and storage tanks [4].

Iron in rural groundwater supplies is a serious problem (levels of 0 to 50 mg/l are found, however the maximum WHO recommended level is not more than 0.3 mg/l. Environmental effects like stains on clothing and bathroom fixtures. Concentration > 0.3 mg/l and reduction in distribution pipes' carrying capacity due to the buildup of bacterial slime and iron oxides gives water and various beverages derived from it a taste that could be described as astringent. Such health effects, the pancreas, liver, spleen, and heart all accumulate excess iron since it is a strong oxidant. Cirrhosis, liver cancer, diabetes, Alzheimer's disease, cardiac arrhythmias, and other bacterial and viral infections are all conditions that can be brought on by it damaging human tissues [5].

Several methods are used to remove heavy metals from aqueous solutions/wastewater include: reduction followed by electrochemical precipitation, chemical precipitation, chemical oxidation–reduction, ultra-filtration, ion exchange, reverse osmosis, solvent extraction, electro-dialysis, electrochemical, coagulation, evaporation and adsorption [6]. The adsorption process is considered as a highly promising technique in comparison to other conventional methods due to its simplicity in operation, flexibility in design, ability to regenerate the sorbent material, cost-effectiveness, high efficiency, and easy compatibility with large-scale application in water and other industries [7].

Now a days there are no appropriate low-cost technologies available for removal of several commonly found groundwater contaminants and the typical conventional water treatment are highly costly and higher amount of chemical sludge is generated which poses disposal problem. Chemical coagulants like Aluminum Sulphate (alum), $FeCl_2$ are used in this conventional drinking water treatment for purification process. But excess use of these chemical coagulants can affect human health e.g., Alum has been indicated to be a causative agent in neurological diseases such as pre-senile dementia and also found to be carcinogenic. To overcome the above-described problem of chemical coagulant problem, it is necessary to increase the use of natural coagulants for drinking water treatment [8]. Natural coagulants that have been tried out as an alternative to inorganic and synthetic coagulants over the years. Inorganic and synthetic coagulants have drawbacks such as lowering pH, increasing expenses, producing a lot of sludge, and being ineffective at coagulating cold water. They also cause Alzheimer's disease and other health issues. On the other hand, natural coagulants offer a number of benefits. Natural coagulants also reduce the amount of sludge produced, and because the sludge they produce is

biodegradable and free of hazardous elements, they can be further valued for use in agronomic applications [9].

Currently, efforts are being made to use readily accessible and affordable agricultural wastes and natural products as adsorbents to remove heavy metals from groundwater and waste water, including sugar cane bagasse, apple waste, coconut shell, orange peel, rice husk, peanut husk, and pecan shells [10]. *Moringa oleifera* (MO) is among these alternatives for wastewater treatment. The filtration of water, industrial uses, and nourishment have all found it valuable. The medium-sized medicinal tree goes by the names "Drumstick" or "Ben oil tree." Africa, South America, and south Asia all have access to it. MO seeds and leaves are frequently employed for the purification of water. No adverse consequences are present. It is a sustainable material that is non-toxic. MOCR (*Moringa oleifera* cake residue) does not require additional processing prior to use in the water purification process [11].

Carbon (graphene, nanotubes) materials can be utilized to make composites that enhance the qualities of biopolymers; graphene and its oxides were added to biopolymers to enhance their mechanical, thermal, and electrical capabilities. The authors created chitosan-chitin nano composites that demonstrated excellent removal of heavy metal ions and dyes. The IR spectra verified the strong connections between the functional groups of the two components. The inclusion of GO improved the thermal stability and mechanical strength of Chitosan films. The antibacterial properties of chitosan were enhanced by composites made of it and GO, which fully prevented the growth of *P. aeruginosa.* To enhance their capabilities for removing iron from ground water, we had also developed a novel, revolutionary material (rGo/MO) composite [12].

1.2. Statement of the problem

It is well known that both the availability and quality of potable water is poor in rural areas of Ethiopia. Endegagn Worada, Gurage zone, is one of rural place in Ethiopia where the community does not have quality water. The water supply coverage of the Woreda is 27 percent (data from Endegagn Woreda water office in 2023) which is below standard level of the country. The water supply in this Woreda and its surrounding areas for cooking, drinking, and other domestic purposes is often directly sourced from ground water without adequate biochemical treatment. The existence of ground water pollutants such as heavy metals especially iron from different sites become increasing from time to time due to increase in natural and anthropogenic

sources of iron in ground water. This causes pollution of water bodies. Elevated amount of iron in shallow well ground water becomes a serious issue in Gurage zone as a whole and particularly in Endegagn Woreda. Almost half of shallow wells are out of service due to this problem. This causes biological, economical and health problem to the community. Even though the case is serious, there was no any study has been conducted previously. There are various methods for removing iron from water. However, most of these technologies are either extremely expensive or too ineffective to reduce metal levels from water [27]. Therefore, it is imperative to synthesis a new and effective adsorptive nano composite material for the removal of elevated iron concentration from the ground water and this study was investigated on it.

1.3. Objectives

1.3.1. General Objective

The main objective of this study is determination and removal of elevated concentration of iron in ground water by using rGO/MO nano composite adsorbent from three sites on Endegagn Woreda, Gurage Zone.

1.3.2. Specific Objectives

The specific objectives of this research were:

- To measure some physiochemical properties of ground water like, turbidity, pH, TH, alkalinity, TDS, EC, TSS.
- To determine concentration of iron using UV-VIS.
- To synthesize rGO, MOSP and their composite for elevated amount of iron removal from ground water
- To characterize the adsorbents using SEM, XRD, FT-IR and UV-Visible spectroscopic techniques

1.4. Significance of the study

This work was intended for the removal of elevated concentration of iron in ground water and make suitable water for cooking, drinking, and other domestic purposes by using MOSP, rGO and their new innovative composite (rGO/MO). This would help to protect the water quality, to make solution regarding health and to intervene in minimizing the economic loss. It would give anticipating information on the level and removal of elevated iron to stakeholders including consumers, Endegagn Woreda water office and concerned body to conduct the required measurement based on the result. It would also serve as a stepping stone and provide background

information on the application of bio sorbents like *moringa olifera* for removal of iron to future researchers.

1.5. Scope of the study

The scope of this study was determined by time and monetary issues. It was focused on the determination and removal of iron only in three shallow well ground water at Endegagn Woreda. It might had been better if larger number of sample sizes and heavy metals included from wider scale to draw a general conclusion. However, due to limited of necessary chemicals and availability of instruments was considered in the study especially, the high cost of instruments, most of which were not available at Wolkite University, seriously limited the scope of this study.

2. REVIEW LITERATURE

2.1. Water and its sources

Water is a liquid at normal conditions, but it often co-exists on earth with its solid state being ice, and gaseous state being water vapor or steam. It has a serious involvement in human lives and daily activities. Human bodies are approximately 60% water, blood is at least 50% water and the human brain made of 77% water. Water can be grouped into Surface water comprising of oceans, rivers, lakes, reservoirs, lagoons, streams and many others, Ground water which is considered mostly as purer than the surface water and lastly the rain water which falls as a result of condensation and precipitation of the clouds. Surface water frequently contains substances that must be removed before it can be used as drinking water while ground water is that pumped from wells and boreholes that have been drilled from underground aquifers and is usually free from harmful contaminants [13].

2.2. Ground water

A well is an excavation or a structure dug, driven, bored, or drilled into the earth to obtain ground water in subsurface aquifers. Well water frequently needs treatment to make it more palatable because it has more minerals in solution than surface water [13]. Groundwater is a major and important source of water for domestic use in both urban and rural settings and is believed to be among the purest forms of water available in nature. According to popular belief, groundwater is cleaner and pollution-free than surface water. However, Residential, municipal, commercial, industrial, and agricultural operations can all have an impact on groundwater quality. It can also become contaminated naturally or as a result of many different sorts of human activity. The site's innate hydrogeological characteristics, agricultural land use, and agricultural production techniques all affect groundwater pollution. Groundwater contamination can result low drinking water quality, a loss of water supply, expensive remediation expenditures, expensive alternative water supplies, and/or significant health issues [14].

2.2.1. Sources of contaminants in ground water

The WHO has developed a useful classification system based on classes of contaminant sources, rather than chemical characteristics. These sources of contaminants include naturally occurring, industrial sources and human dwellings, agricultural activities, water treatment or materials in contact with drinking water, Pesticides used in water for public health purposes and Cyanobacteria [15].

Chemical unique properties of water due to its polarization and hydrogen bonds which resources it is able to different combinations to suspended, dissolve, absorb in natural water, is unclear as it obtains pollutants from its nearby and individuals rising from people and animals as health as other biochemical actions. The environmental contaminations by the toxic substances are growing that cause major concern to the local users. An extensive area of pollutants is constantly introduced into the aquatic environment primarily due to amplified industrial activity, technical development, growing human population and mistreatment of natural resources, agriculture and domestic wastes run-off. These pollutants, heavy metals found one of the most hazardous since of their stubborn nature, tendency, toxicity to accrue in organisms and undergo food chain increase and more still, they are non-degradable [15].

2.2.2. Heavy metals contamination of ground water

Heavy metal pollution of the environment has become a growing ecological crisis and concern and therefore the subject of many researches. These heavy metals are continuously released into the aquatic environment from natural process like volcanic activity and weathering of rocks. Industrial processes like electro plating, metal finishing, metallurgical, chemical manufacturing and mining industries have greatly enhanced the concentration of heavy metals in the water [16]. Ground water contains elevated concentrations of iron, arsenic, fluoride, radioactive elements and nitrates due to natural processes as well as human activities like seepages from underground storage facilities and faulty septic systems. Trace metals are contaminants due to their toxicity potentials at very low concentrations and tendency to bio accumulate in tissues of living organisms over time. They gain entrance into human systems by contaminated drinking water, food and air. After its entrance to the body, the bioavailable form of these metals can compete with, and displace essential minerals such as zinc, copper, magnesium and calcium; and interfere with organ system function. Toxic metals such as mercury (Hg), cadmium (Cd), arsenic (As), chromium (Cr), thallium (Tl) and lead (Pb) have no beneficial effects in humans, as such long-term exposure may cause more severe disruptions in the normal functioning of the organ systems where the metals are accumulated. Pb, for example, is associated with a wide range of negative pregnancy outcomes, including early membrane rupture and spontaneous abortion, erectile dysfunction, and contributes to cardiovascular diseases. Metals such as As, Mn, Ti, Cd, Cr, V, Co, Cu, Fe, Pb, Ni, Zn and their compounds have been shown to be initiators or promoters of

carcinogenic activity in animals. Also, Be, Sb, Al, Hg, Ni, Cd and Co can cause adverse reproductive/fertility problems [17].

2.3. Iron

Iron which is the fourth most abundant element and second most abundant metal in the earth's crust is a common constituent of groundwater.

2.3.1. Some Physical and chemical property of iron

When pure, iron is a silvery-white metal that is notable for its capacity to absorb and hold magnetic fields as well as its capacity to dissolve minute amounts of carbon when melted (producing steel as a result). The heating of Fe_2O_3 (hematite) or Fe_3O_4 (magnetite) with a mixture of other materials in the high temperature environment of the blast furnace provides the basis for commercial iron refining. To pure iron, the oxides are reduced. Pure iron corrodes destructively when exposed to oxygen and moisture in the environment. Even alloys like steel require painting or other forms of coating for protection. [18].

The divalent ferrous ion (Fe^{+2}) able to oxidized in to trivalent ferric ions (Fe^{+3}) as;

$$Fe^{+2} = Fe^{+3} + e^{-}$$

Where high concentration of dissolved oxygen occurs, the trivalent ferric ion can further react with hydroxyl groups to precipitate in solid form

$$Fe^{+3} + 3OH^{-} = Fe(OH)_3 \quad \text{..... Eq. 1}$$

And whole oxidation-reduction reaction can be written as

$$Fe^{+2} + 3H_2O = Fe(OH)_3 + 3H^{+} + e \quad \text{..... Eq. 2}$$

Hydrogen gas is produced when iron combines with extremely hot water and steam. Additionally, it disperses in the majority of acids and undergoes reactions with a wide range of other substances. Divalent ferrous iron Fe^{+2} (soluble form) and trivalent ferric iron Fe^{+3} (insoluble form) can both be found in water supplies.

The stability of ion is dependent on pH and redox potential. Mostly in ground water iron originated from withering of iron ores like pyrite. Through the Weathering of pyrite in heaps of pit coal, reduced groundwater with a content of Fe^{+2} originates as in the following reaction.

$2FeS_2 + 7O_2 + 2H_2O = 2Fe^{2+} + 4SO_4^{-} + 4H^{+}$…….... Eq.3

$5FeS_2 + 14NO_3^{-} + 4CO_2 + 2H_2O = 5Fe^{2+} + 10(SO_4)_2^{-} + 7N_2 + 4HCO_3^{-}$ (1) ……..Eq.4

Free iron ions form complexes with water in aqueous solutions. The simplest of these complex ions are: the hexa aquairon (II) ion: $[Fe(H_2O)_6]^{2+}$ the hexa aquairon(III) ion: $[Fe(H_2O)_6]^{3+}$ They are both acidic ions, but the iron (III) ion is more acidic [18].

2.3.2 Sources of iron in ground water

Iron is a common metallic element found in the earth's crust. The presence of iron in ground water is a direct result of its natural existence in underground rock formations and precipitation water that infiltrates through these formations. Since the earth's underground rock formations contain about 5% iron. Water percolating through soil and rock can dissolve minerals containing iron and hold them in solution. Occasionally, iron pipes, well casing, pump parts, and storage tank also may be a source of iron in water. The main anthropogenic sources of Iron are various industrial effluent sources, mining activities (acid mine drainage), landfill leakages, Power plants combustion, etc. [19].

Natural sources of iron may include weathering of iron bearing minerals like amphibole, iron sulfide and iron rich clay minerals. In areas where groundwater flows through an organic rich soil, iron will also dissolve in the groundwater. During the Weathering of pyrite in heaps of pit coal, reduced groundwater with a content of Fe^{+2} originates. [20].

Table 1: Important Iron minerals [20]

Olivin	$(Mg, Fe)_2 SiO_4$
Magnetite	Fe_3O_4
Chromit	$FeCrO_4$
Ilmenite	$FeTiO_3$
Pyrrhotit	FeS (in meteorites Troilit)
Pyrite	FeS_2
Hamatit	Fe_2O_3, Fe_2O_3- hydrate
Geothit	α-FeOOH
Lepidokrokit	γ-FeOOH
Iron Carbonate	$FeCO_3$
Vivianit	$Fe_3(PO_4)_2.8H_2O$
Strengit	$FePO_4.2H_2O$

2.3.3. Types/forms/ of iron in ground water

Two major types of iron can be found in water. These are clear-water iron (ferrous iron) and red-water iron (ferric iron).

Clear-water iron (ferrous iron): The most frequent type which generates the most complaints from water consumers. Iron dissolves in low oxygen environments, such as deep wells or aquifers, and the water remains pure and colorless. Even though tap water may appear clean, if it is left to stand for a while, rust-colored particles may start to develop and sink to the bottom.

Red-water iron (ferric iron): When exposed to the atmosphere, ferrous iron begins to oxidize and reddish-brown-to-black particles begin to form. This "rusty "sediment is the ferric form of iron. Ferric iron is insoluble in water. Iron is mainly mobilized and redistributed during weathering of the igneous and metamorphic rocks. However, the process of mobilization and redistribution occur in the form of either dissolved Fe^{2+} or solid particles of Fe (III) oxyhydroxides in an environment void of oxygen or where oxygen is present, respectively. When groundwater is abstracted to the surface or in surface water, Fe is usually found in the precipitated ferric form Fe (III) and often associated with suspended solids [21].

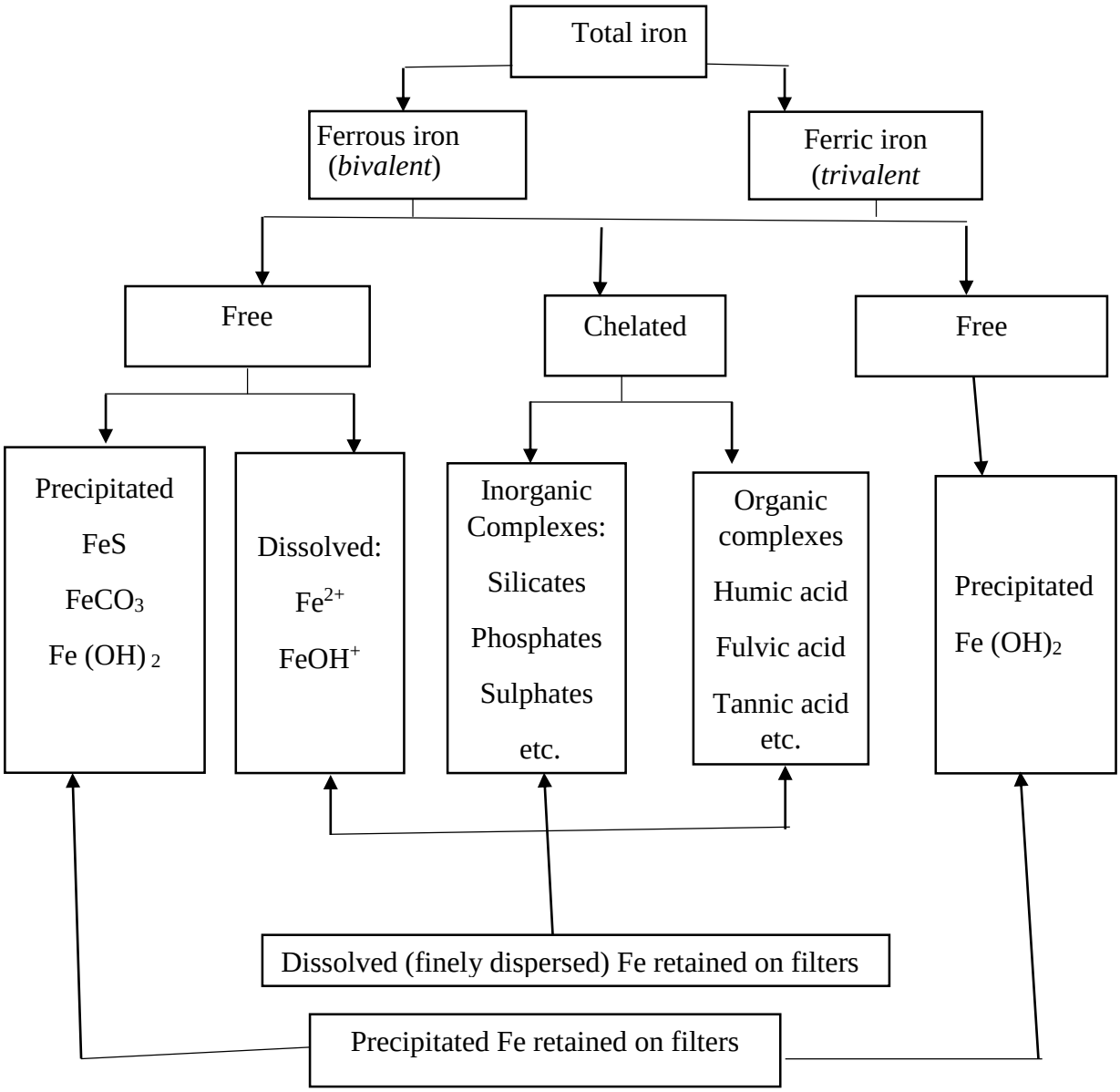

Figure 1: Forms of iron in ground water [21].

2.3.4. Health effects of elevated iron in water

Excess iron (the presence of iron (Fe) content that exceeds the threshold (0.3 ppm) can increase production of reactive oxygen species, resulting in oxidative stress cascades that lead to lipid oxidation and DNA damage. Aberrant iron accumulation is implicated in aging and in several diseases, including cardiovascular diseases, neurodegenerative diseases, and cancer. It can also cause health problems or disorders such as damage to the intestinal wall and decreased lung function. Water soluble binary iron compounds such as $FeCl_2$ and $FeSO_4$ may cause toxic effects

upon concentrations exceeding 200 mg, and are lethal for adults upon doses of 10-50 g. A number of iron chelates may be toxic, and the nerve toxin iron penta carbonyl is known for its strong toxic mechanism. Iron dust may lung disease [22].

Iron is a strong oxidizer and excess amount is stored in pancreas, liver, spleen and heart. It able to damage body tissues which causes Cirrhosis, Liver cancer, Cardiac arrhythmias, Diabetes, Alzheimer's disease and different bacterial and viral infections [5].

2.3.5. Disadvantages of iron in water

Water containing high concentrations of iron is objectionable owing to the production of dis colorations, turbidity, deposit and taste. The water may react with tannins in coffee, tea and other beverages to produce a black sludge. Water in wells may similarly acquire an inky color owing to the combination of iron and tannin derived from trees, particularly oaks. Even small traces of iron in water lead to accumulation of appreciable deposits in distribution mains and reservoirs, and these often prove troublesome to water authority and consumers hence the need for periodical main-flushing. Water containing iron is also not suitable for many industrial purposes such as paper-making, dyeing, photographic film manufacture and ice-making [23, 6].

2.3.6. Advantages of iron in water

Iron is a common building material, including for drinking water pipes. Paints and plastics contain iron oxides as pigments. Other substances are used to treat iron deficiency in humans and as food coloring. As coagulants, several iron salts are employed in the treatment of water. The majority of plants and animals require it at the proper concentration in water for nutrition and healthy development [23].

2.4. Determination of iron concentration in water

The amount of iron in water has been determined using a variety of analytical techniques. They include HPLC techniques, which allow for the possibility of multi-element analysis by separating distinct iron and other cation complexes. The drawback of these procedures is the requirement for sample pre-treatment, such as solid phase extraction or solvent extraction. Different spectrophotometric techniques have also been used; some of them combine flow injection analysis with them. Iron in water and other cations have also been determined using inductively coupled with plasma spectrometry. For the simultaneous determination of EDTA-Fe (III) and free EDTA, iron has been separated by capillary isotachophoresis as an EDTA

complex, rather than in water, but in wash solutions used for the desulfurization of gases. Furthermore, in analytical chemistry, special attention is given to development of methods simultaneously combining preconcentration and determination. Methods are continually being developed to improve the selectivity, sensitivity and specificity of an analyte. It is equally important to consider new methods in terms of cost, convenience and the number of samples throughout. The precision and accuracy of methods are also critical factors in any analysis [24].

2.4.1. UV-VIS spectrometry

UV-VIS spectroscopy method is a promising way and a highly sensitive, easy and accurate technique for the determination of trace amounts of metals in solution.it was the standard method for the determination of ferrous iron concentration and its removal techniques. This study was important for regular monitoring of Fe^{2+} concentrations in the real samples of ground water. The instrumentation technique consists of three principal components. Light source which holds, (tungsten-iodine lump near UV–VIS to IR region in the range of 380-1000 nm and deuterium discharge lump, also for UV region is in the range of 200 –380 nm), beam splitter, sample holder (reference cell and sample cell), detector, display ratio. The solution with analyte is directly exposed to the light and corresponding absorption of the characteristics wavelength of peak generates. During this step a maximize amount of metal deposited can be produced from the peak absorbance of characteristics wave length at about 510nm for Fe (II) [25].

The UV region ranges from 190 to 400 nm and the visible region from 400 to 800 nm. The technique can be used in both quantitative and qualitative determination for further analysis of research and development works. Also in modern applications of UV-visible spectroscopy is a technique that readily allows determining the concentrations of substances. As such UV –VIS spectroscopy is used extensively in academics, research and health care analytical laboratories for the quantitative analysis of all molecules through which ultraviolet and visible electromagnetic radiation absorbs [25].

1, 10-phenanthroline, or o-phenanthroline, serves as the ligand to create a colorful complex. Only the compound o-phenanthroline may cause Fe^{+2} to react, and this compound absorbs in the visible spectrum (at about 510 nm). In acidic environments, this process takes place. The complex's formation solution was buffered with sodium acetate and protected from oxidation with hydroxylamine HCl. How soluble iron is formed

$4Fe^{3+}(aq) + 2\ NH_2OH(aq) \rightarrow 4\ Fe^{2+}(aq) + N_2O(aq) + 4\ H^+\ (aq) + H_2O(l)$…….. Eq. 5

$Fe^{2+}\ (aq) + 3\ C_{12}H_2N_2\ (aq) \rightarrow [(C_{12}H_2N_2)3Fe]^{2+}(aq)$ ……..... Eq. 6

an orange-red complex is the result of the interaction of Fe^{2+} with $C_{12}H_2N_2$ (l) (o-phenanthroline). A calibration curve was created following colorimetric measurements on various solution concentrations. Iron was also examined in a substance that was unknown. It is possible to calculate the absorption of an unknown substance and an iron supplement using the Beer-Lambert Law (A=bc) [26].

2.5. Removal of elevated iron from ground water

Iron removal from groundwater is a major concern for most scientific researchers. There are various methods for removing iron from water including ion exchange, oxidation by oxidizing agents, chemical precipitation, supercritical fluid extraction and accumulation by aquatic macrophyte. However, most of these technologies are either extremely expensive or too ineffective to reduce metal levels from water. In this context, we would have chosen the iron removal method of ground water by adsorption on MO, rGO and their composite (rGO/MO). The adsorption process has many advantages such as: low cost of adsorbent, easy application, use of natural, domestic and industrial waste as adsorbents [27].

2.5.1. Adsorption

Adsorption is the adhesion of an adsorbate such as a fluid, liquid, or gas, by creating a thin layer or film on the surface of an adsorbent whether it is a solid or liquid. The bonding between adsorbate and adsorbent could be physical or chemical bonding. The chemical bonding provides stronger bonding than physical bonding, and the film might be single or multiple layers. Adsorbate can be separated from the adsorbent and the process is called desorption [28].

2.5.1.1. Types of adsorptions

The interfacial layer mechanism can be explained by two principles:-

Physical Adsorption, also known as physisorption, refers to a bonding process in which neither the substrate nor the sorbent's chemical structure is altered. **Chemical Adsorption**, also known as chemisorption, is the development of a chemical link between a substrate and an adsorbent as a result of a rearrangement of electron density between the two. This bond may be an ionic or covalent bond [29].

2.5.2. Adsorbents

Natural coagulants are the best alternatives than the use of inorganic and synthetic coagulants. The demerits of using inorganic and synthetic coagulants are it causes Alzheimer's disease and similar health related problems, reduction of pH, high costs, production of large sludge volume and low efficiency in coagulation of cold water. Natural coagulants, however, provide a number of benefits because of their relative low cost, they allow for less sludge production, and the resulting sludge is biodegradable and contains no hazardous elements, allowing for further valorization in agricultural applications [9].Currently efforts have been made to use cheap and available agricultural wastes/Natural products such as sugar cane bagasse, coconut shell, orange peel, rice husk, peanut husk, pecan shells, jackfruit, maize cob, apple waste and sawdust as adsorbents to remove heavy metals from Ground water/waste water [10].

2.5.2.1. *Moringa oleifera*

The *Moringa oleifera* tree, which serves a variety of purposes, is a member of the *Moringaceae* family, which consists of 13 varieties of plants. Asia, sub-Saharan Africa, and Latin America are all home to this tropical plant. Most of the plant's parts are used for useful uses in MO, which is a well-known example of a tree. MO is occasionally known to as the miracle tree because to the wide range of uses it has. Due to its drought tolerance, the MO tree is commonly utilized as a vegetable, medicinal plant, dietary supplement, livestock feed, fertilizer, and a source of oil in underdeveloped countries. The seeds of the *Moringa oleifera* plant contain 40% oil by weight, which can be utilized for producing, cooking, and lighting. [30].

Figure 2: *Moringa oleifera* tree with pods and seed kernels [30]

1. *Moringa olifera seed*

Moringa oleifera seeds have a brownish semi-permeable seed hull, with 3 papery wings. About 15000 to 25000 seeds can be produce in each tree per year. Average weight is 0.3 mg/seed. The

seeds contains 4-benzyl isothiocyanates,4-phenyl acetonitrile, 4-hydroxyphenylacetonitrile, and 4-hydroxyphenyl-acetamide, 4-benzylglucosinolate Roridin E, Veridifiorol, 9-Octadecenoic acid, 0-ethyl-4-benzyl carbamate, niazimicin, niazirin, beta- sitosterol, glycerol, 3-O-beta-sitosterol and beta-sitosterol-3- O-beta-D-glucopyranoside., An active antimicrobial agent ascribed to plant synthesized derivatives of benzyl isothiocyanates known as 4- benzyl isothiocyanates was identified from earlier researches and about 8-10% of this compound is present in both defatted (after removing oil) seed and crude seed. The advantages of *Moringa oleifera* as coagulant: Cheap and easy method for developing countries (especially at household level), the processing doesn't modify the pH of the water, it doesn't alter the water taste (unless a very high dose is added). But the treatment water with *Moringa oleifera* coagulant does not completely removal microbes which promotes secondary bacterial growth after the water coagulation [31].

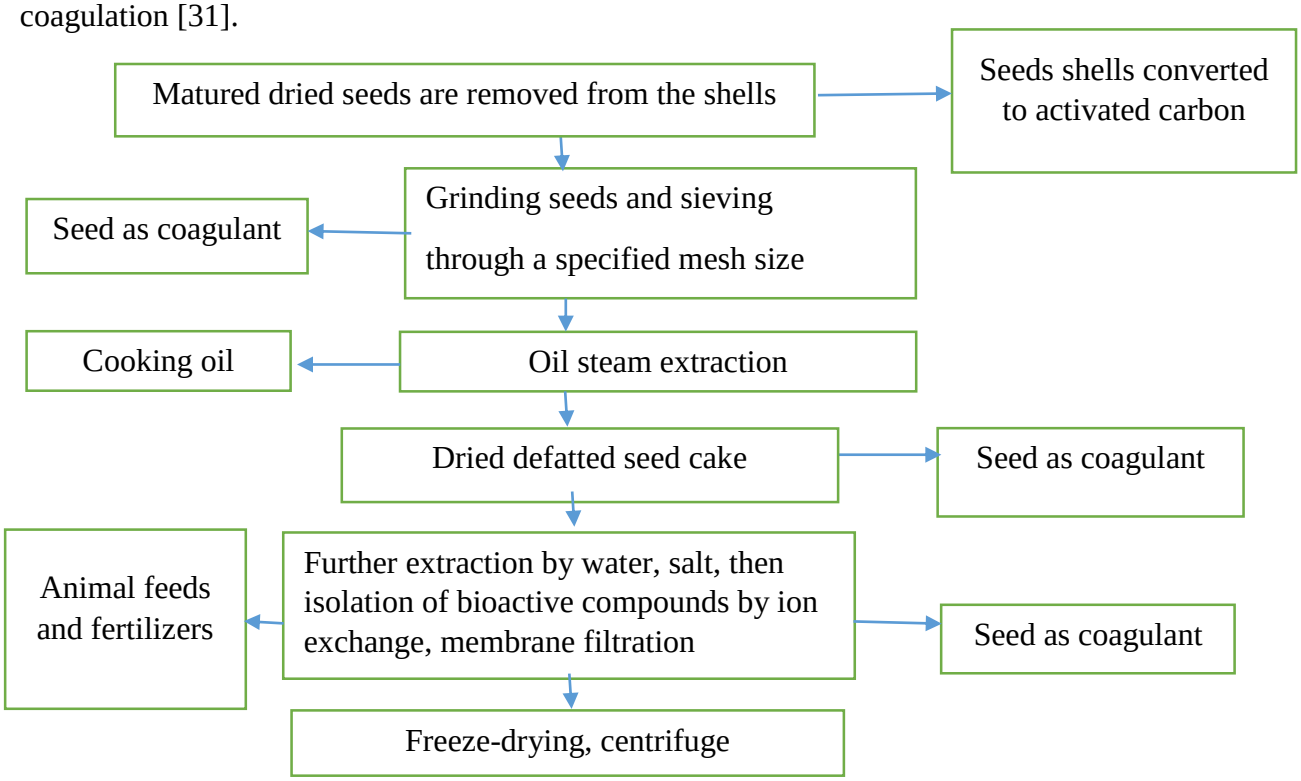

Figure 3: A flow chart diagram showing *Moringa oleifera* seed coagulant processing techniques [31].

Parts of *Moringa oleifera* plants have been reported to various phytochemical parameters; it is a good source of antioxidants, including quercetin and chlorogenic acids, such as flavonoids, phenolics, astragalin, anthocyanins, cinnamates, and carotenoids, as well as a rich source

ofcarotene,K, Ca, terpenes, quinines, saponins, alkaloids, proteins, tannins, and vitamin C, thus improving the shelf life of fat-containing foods, act as a good metal reducing, capping, and stabilizing agent [32].

2.5.2.2. Graphene oxide (GO)

Graphene oxide (GO) is the most important graphene adsorbent, due to its low cost and high performance. Graphene is a one-atom-thick planar layer of sp2 hybridization carbon atoms which arrange in a hexagonal structure. It has unique and remarkable mechanical, thermal, optical, and electrical properties. In addition, the two-dimensional structure causes graphene to have a zero-band gap and to act as a semimetal [33].

Graphene oxide (GO) is one of the most prominent of nano scaled membranes for water purification. GO sheets have hexagonal structure as pristine graphene, but with oxygen-based functionalized sites. It shows high electronic mobility, thermal conductivity, and remarkable mechanical strength, with the advantage of being highly stable in water. As well, its surface can be easily functionalized by organic biomolecules, strong π–π stacking and VDW interactions [34].

GO has two important characteristics: (i) It can be produced using inexpensive graphite as the raw material and by using cost-effective chemical methods with a high yield and (ii) It is highly hydrophilic and can form stable aqueous colloids to facilitate the assembly of macroscopic structures by simple and cheap solution processes. The graphene sheet consists of only trigonally bonded sp2 carbon atoms and is perfectly flat apart from its microscopic ripples. In terms of electrical conductivity, GO is often described as an electrical insulator because of the disruption of its sp2 bonding networks. To recover the honeycomb hexagonal lattice, and with it the electrical conductivity, the reduction of GO has to be achieved. Functionalization of GO can fundamentally change the properties of GO. The resulting chemically modified graphenes could then potentially become much more adaptable for many applications [35].

2.5.2.3. GO preparation

Graphene can be synthesized by various methods such as chemical vapor deposition, mechanical exfoliation and cleavage, and annealing a single-crystal Sic under ultrahigh vacuum. These methods, however, have many disadvantages including high energy requirement, low yield, and limitation of instrument. Up to now, the chemical method is simple, inexpensive, and suitable

for large-scale or mass production of graphene sheets, although graphene derived by this method could contain a significant amount of oxygen functional groups and defects [33].

A GO compound can be obtained through chemical oxidation of carbon sources, such as graphite, using oxidizing agents (e.g., $KMnO_4$, H_2SO_4 etc.) to produce graphite oxide. Then, distinct exfoliation methods can be used to yield GO nano sheets. The possibility of large-scale production of GO makes it inexpensive in comparison with other materials [34].

2.5.2.4. Some physical and chemical properties of reduced graphene oxide

Reduced Graphene Oxide has robust features and auspicious functionalities as compared to Graphene Oxide like more efficient optical properties, better electron mobility, physiochemical stability, excellent bond, good surface area, high thermal-conductivity, and great resilience. Reduced Graphene Oxide have the ability to be as co catalyst when reacted with TiO_2 that aims to improve photo catalyst redox capabilities under visual in addition to UV radiation source. Regarding its outstanding electronic conductivity, it has the ability to separate photo generated electrons to override the electron hole reinstallation rate. Nevertheless, the results show that π-π interactivity with organic dyestuff stuffs and formulization of hydrogen connecting all organic pollutants, improves the photo catalyst degeneration procedures [36].

2.5.2.5. Preparation of reduced graphene oxide

Reduced graphene has fewer oxygen atoms, thus, is less negatively charged. Reduced graphene is another important graphene adsorbent. There are two major routes to prepare reduced graphene, namely, the direct growth and the chemical reduction of GO. In the adsorption studies, the chemical reduction of GO is widely used because it is easy, is low-cost, and has a high throughput [37].

2.5.3. Factors affecting adsorption

2.5.3.1. pH Effect

The pH of the solution is one of the most important factors affecting the adsorption and ionic exchange processes. In the case of surfaces containing polarized or charged locations, the amount of adsorption increases if the surface acquires a charge that exceeds the charge of the minutes absorbed by the effect of acidity. Conversely, the amount of adsorption decreases if the surface and the evaporated minutes acquire a similar charge [38].

2.5.3.2. Initial concentration Effect

The adsorption process is affected by the primary concentration of the adsorbent material because the largest amount of ions or absorbable molecules is exposed to the active sites in the adsorbent at the high concentration, which increases the adsorption speed while the percentage of adsorption.

2.5.3.3 Nature of Adsorbate

The size of the ion plays an important role in the adsorption process, affecting the amount of adsorption of a certain ion on the surface of the atom with the presence of more than one ion of different size in the solution. The solubility of the adsorbent in the solvent also has an effect on the adsorption process where the amount of the adsorbent is reduced by increasing its solubility in the solvent. The soluble solubility is increased and the adsorption of the solvent [38].

2.5.3.4. The Effect of Adsorbent Dose

Removal percentage of metal ions increased when adsorbent dosage increases. Increased the amount of adsorbent in adsorption of five different types of heavy metals. However, performance enhancement is only for several additions in adsorbent dosage, and after certain value the performance will gradually become constant and does not have notable increment. Increase in adsorbent dosage indicates more surface area available for adsorption and greater adsorption sites. When adsorbent dosage is below the optimum value, the removal of metal ions is low due to lower binding sites available for adsorption.

2.5.3.5. The Effect of Contact Time

Contact time demonstrated the removal percentage of metal ions from solution with respect to the time. Initially, the rate of adsorption will increase significantly and gradually reaching equilibrium. It varies depending on type of adsorbent and pollutant itself. After reaching its optimal point of contact time, equilibrium concentration does not have a significant change. Increasing the contact time, no further adsorption was observed as remaining metal ions became asymptotic with time axis [39].

2.5.4. Batch adsorption study

The batch adsorption study was used to access the adsorption capacity of adsorbent. The amount of metal ion adsorbed onto adsorbent was determined by using following equation.

$$Q_t = (C_i - C_e/W) \times V \quad \text{..... Eq.7}$$

Where, Ci = Initial concentration of metal ion (mg/L), W = Weight of adsorbent (g).

Ce = Equilibrium concentration of metal ion (mg/L). Qt = Amount of metal ion adsorbed onto adsorbent at time‘t’ (mg/g), V = Volume of metal ion solution (L)

Likewise metal ion removal percentage was calculated by using the following equation.

$R\% = (C_i - C_e/C_i) \times 100$ . . . . Eq.8 [40].

2.5.4.1. Adsorption isotherms models

In general, an adsorption isotherm is an invaluable curve describing the phenomenon governing the retention (or release) or mobility of a substance from the aqueous porous media or aquatic environments to a solid-phase at a constant temperature and pH. Adsorption equilibrium (the ratio between the adsorbed amount with the remaining in the solution) is established when an adsorbate containing phase has been contacted with the adsorbent for sufficient time, with its adsorbate concentration in the bulk solution is in a dynamic balance with the interface concentration. Typically, the mathematical correlation, which constitutes an important role towards the modeling analysis, operational design and applicable practice of the adsorption systems, is usually depicted by graphically expressing the solid-phase against its residual concentration [41].Langmuir and Freundlich isotherm were employed to investigate the adsorption behavior.

2.5.4.2. Langmuir isotherm equation

Is determined by: qe = qm ka Ce / (1+ ka Ce). …... Eq.9

Where: Iron adsorbed per unit mass at equilibrium (mg/g), according to question qe

The maximum amount of iron that may be absorbed per unit mass of adsorbent (mg/g) is the definition of the quantity. Ce: Adsorbate concentration (mg/l) in the solution at equilibrium the equilibrium constant is Ka.

Equation (9) can be expressed linearly as $Ce / qe = 1/ (Ka\ q_m) + Ce / q_m$….. Eq.10

The dimension-less separation factor, or RL, which is defined as RL = 1/ (1+ Ka Co)... Eq.11 can be used to represent the fundamental properties of the Langmuir isotherm. RL: Dimension less separation factor The Langmuir constant is Ka. Co: The iron content at the start (mg/l) [42].

2.5.4.3. Freundlich Isotherm Model

Freundlich adsorption isotherm model is a type of isotherm model in which the absorbents form a monomolecular layer on the surface of the absorbent, but unlike the Langmuir model, application to multilayer adsorption is also possible. The Freundlich model expression shows the heterogeneity of the surface of the molecules as well as the exponential distribution of active sites and their energies. The non-linearized form of Freundlich isotherm model expression the linearized form is shown in Equation $Qe = KFCe\ 1/n$ $In\ Qe = ln\ KF + 1n\ In\ Ce$... Eq. 12 where KF is the Freundlich constant or maximum absorption capacity (L/mg), n is the adsorption intensity or surface heterogeneity, which indicates the energy distribution and the absorbate site's heterogeneity [43].

3. MATERIALS AND METHODS

3.1. Description of the study area

Endegagn Woreda is found in Gurage zone Southern Nations, Nationalities, and Peoples Regional state of Ethiopia. Dinkula is the town of Endegn Woreda, which is 230 kms away from Addis Ababa (capital city of Ethiopia), 277 kms from Hawasa (administrative city of Sidama Region), and 75 kms from Wolkite (Gurage zone town). The size of the Woreda is 127 sq. kms, which is the smallest of all other Woredas of Gurage Zone. The Woreda is bordered by Enemor and Ener Woreda to the North and to the West, Geta Woreda to the North East, Hadiya Zone to the West and South West, and Silti Zone to the East and South East. Administratively, the Woreda is divided in to 17 rural Kebeles and one urban Kebele. Each Kebele has 10 or more villages with different local names. The study was conducted in this Woreda within 3 kebeles (such as Welecho, Zigaz and Araticho) which have shallow well water supply by taking one shallow well in each kebeles.

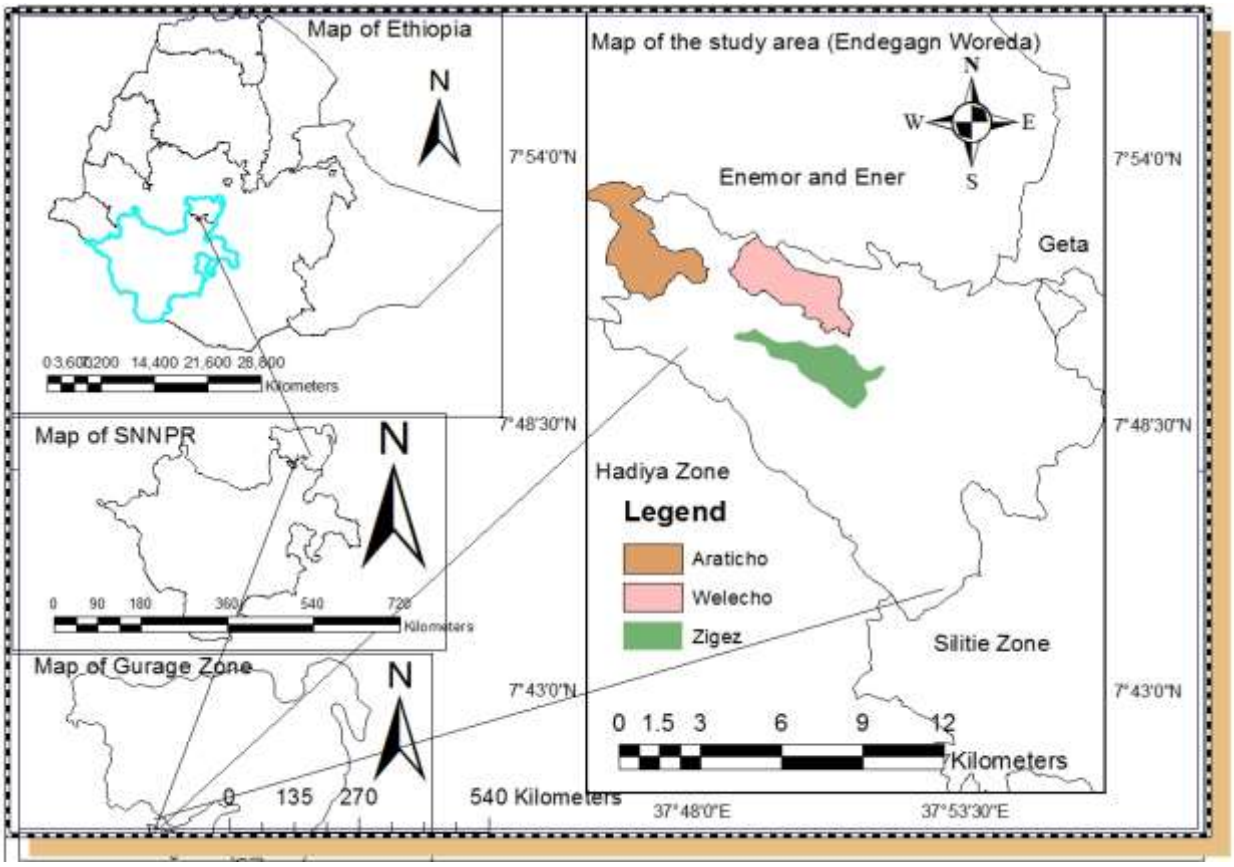

Figure 4: Map of the study area

Source: Owen construction from shape file (2023)

3.2. Chemicals

All chemicals were in analytical reagent grade and used without further purification. Ferrous ammonium sulphate $(NH_4)_2Fe(SO_{4)2}.6H_2O$), natural graphite (99%) supplied by Aldrich, potassium permanganate ($KMnO_4$), 98% sulfuric acid (H_2SO_4),sodium hydroxide(NaOH),hydrochloric acid (HCl), and 30% hydrogen peroxide (H_2O_2), sodium nitrate ($NaNO_3$), ascorbic acid, nitric acid (HNO_3), EDTA,$AgNO_3$, Erichrome black T indicator, potassium chromate indicator, Hydroxylamine Hydrochloride $[NH_3OH]^+Cl^-$, 1,10 Phenonthroline ($C_{12}H_8N_{2)}$, Sodium acetate ($C_2H_2NaO_2$) and distilled water.

3.3. Instruments and Apparatus.

Polyethylene plastic sample holder, ice bath refrigerator, Oven dryer, Electronic Analytical balance, mortar and pestle, Centrifuge, pH meter, thermometer, conductivity meter, Stirrer, measuring cylinder, dropper, pipette, volumetric flask, Micro Pipette, quartz cuvete, funnels, filter paper, beaker, AAS or UV-VIS, SEM, FTIR and XRD

3.4. Experiment sites

Ground water collected from three shallow wells was characterized based on the physicochemical parameters like pH, turbidity, electric conductivity, total suspended solid (TSS) and total dissolved solid (TDS), chloride, alkalinity, Hardness etc. which were conducted in the chemistry laboratory of Wolkite University and Gubrie Zebidar Beer Factory (BGI).Reduced graphene oxide with moringa oleifera seed powder were synthesized and their removal of elevated Fe^{2+} concentration from ground water was evaluated in WKU analytical chemistry laboratory. Some characterizations were performed in different places due to the lack of instruments in WKU; Characterization by SEM was analyzed at the Adama Science and Technolology University, whereas XRD, UV-visible and FTIR were done at Addis Ababa University.

3.5. Sample collection

Three shallow well water samples were collected from Welecho, Zigaze and Araticho kebeles, Endegagn Woreda. Randomly one shallow well was taken in each kebeles. The raw ground water was collected using washed and rinsed polyethylene plastic bottles from a source of these selected area by first pouring it for 5 seconds to get a representative sample. Then it was acidified

with 2 ml of nitric acid to stabilize the pH and to prevent iron from precipitation before analysis in the laboratory. Finally, it was stored at 4°C refrigerator until analysis.

3.5.1 Cleansing of sampling materials

All the polyethylene bottles were entirely washed with tap water and detergents, rinsed with distilled water and soaked in 10% (v/v) HNO_3 for about 24 hrs. Next to that, all containers were rinsed with distilled water, dried and kept in dust free place to avoid contamination. The containers were rinsed with sample water prior to actual sample collection before using for sampling.

3.5.2. Collection and refining of *Moringa olifera* seeds

Dry *Moringa Olifera* seeds was collected from Abeshge Woreda Wudad 5 kebele, in Gurage Zone and stored at room temperature prior to use. The seeds were unshelled, and the kernels were washed with plentiful amounts of deionized water to remove any sticking dirt before drying in the oven at 65 ˚C for 24 h. The dried samples were grounded using mortar and pestle and sieved to obtain a fine powder small mesh size and kept for adsorption studies. A part of the powder was characterized by XRD, FT-IR, SEM and UV-Vis spectroscopy.

3.6. Sample preparation

All the ground water samples, synthetic water samples and adsorbent samples were prepared before analyzed as follows.

3.6.1. Digestions of ground water samples for heavy metal determination

Acid digestion using 69 % nitric acid were performed to destroy organic matter and to dissolve larger particles in the sample, thus allowing determination of the total concentration of the metal. A final addition of 2 mL of nitric acid was added to all samples in order to dissolve any remaining particles. Each of the digested water samples was filtered through whatman filter paper No.42 in to a 100mL volumetric flask and filled up to the mark with distilled water. The concentrations of heavy metal (iron) was determined using UV-VIS.

3.6.2. Preparation of graphene oxide using Hummer's method of synthesis

The graphene oxide was prepared by using the Hummer method with little modification. Accordingly, 5 gm graphite powder and 2.5 gm sodium nitrate were mixed with 120 mL of 98% sulfuric acid in 1000 mL of the conical flask. The mixture was stirred for 30 min in an ice bath followed by the addition of 12 gm potassium permanganate with vigorous stirring at a temperature of below 20°C. The stirring continued overnight and 150 mL of distilled water was

slowly added to terminate the reaction. The reaction temperature was rapidly increased to 98°C and 50 mL of 30% H_2O_2 was added. Then the product sample was washed with 5% HCl, deionized water, and then finally dried in oven at 60 °C [47].

3.6.3. Preparation of reduced graphene oxide

GO prepared by Hummer's method consists of a-few-layer carbon platelets decorated with oxygen containing functional groups. The removal of some oxygen-based groups by reducing agents or thermal treatment can yield rGO. GO can be exfoliated via ultra-sonication and then reduced by hydrazine hydrate, a strong reducing agent, for 2 hrs. Since hydrazine is toxic, alternative reagents such as $NaBH_4$, ascorbic acid, and HI can be used. Among these, ascorbic acid was used essential for the scalable production of rGO and did not produce toxic gases [48].

3.6.3.1. Reduction of GO using L-ascorbic acid

50 mg GO (0.1 mg/ml) was dispersed in distilled water via sonication for 45 min. 0.1M L-ascorbic acid was dissolved in distilled water. The obtained mixture of GO and L-ascorbic acid (1:1 volume ratio) was homogenized using magnetic stirrer at 60°C for 1 hour. The color of the mixture changes from brown to black. The mixture was centrifuged at 4000 rpm for 10 min. 10 ml of 30 % H_2O_2 was added to the mixture in order to remove remaining ascorbic acid. The mixture was sonicated for 30 minutes at 60°C. The mixture was repeatedly washed with distilled water and ethanol. The product was centrifuged at 4000 rpm for 20 min and dried at 100°C in oven [49].

3.6.4. Preparation of MOSP and rGO composite

Composite of MOSP and rGO was prepared by adding 5g MOSP in 1:1 ratio to the graphite powder at the beginning of the procedure used for the preparation of GO. Accordingly, 5 gm MOSP, 5gm graphite powder and 2.5 gm sodium nitrate were mixed with 120 mL of 98% sulfuric acid in 1000 mL of the conical flask. The mixture was stirred for 45 min in an ice bath followed by the addition of 12 gm potassium permanganate with vigorous stirring at a temperature of below 20°C. The stirring continued overnight and 150 mL of distilled water was slowly added. The reaction temperature was rapidly increased to 98°C and 50 mL of 30% H_2O_2 was added. Then the product sample was washed with 5% HCl, deionized water, and then finally dried in oven at 60 °C [47].

3.6.5. Iron standard Solution preparation

5, 10, 15 and 20 ppm of standard iron solution were prepared from 1000 ppm of iron solution by diluting with deionized water in 100 mL of volumetric flask [50].

3.7. Sample Analysis

The initial and final concentration of Fe^{2+} in all samples of ground water was measured by UV-visible spectrometer. Each standard solution at different concentrations were prepared from stock solution which was used to get calibration curve for the metal. The pH and temperature of the sample were measured using portable pH meter and thermometer on site and in the laboratory. The other parameters like TDS, TSS, hardness, turbidity, alkalinity, and chloride of the samples were analyzed at Organic Chemistry laboratory in WKU and Gubrie BGI Ethiopia brewery factory. The measured values were compared to WHO guidelines and Ethiopia guideline values used as reference sources [44, 45, 46].

3.7.1. Characterization of MOSP, rGO and rGO/MO adsorbents

3.7.1.1. Fourier Transforms Infrared (FT-IR) Spectroscopy

An FTIR spectrum is a useful tool commonly used to identify functional groups that are attached to a certain surface. It was used to analyze the chemical structure spectra of moringa oleifera (MO), reduced graphene oxide (rGO), and their composite (rGO/MO) samples. The FTIR spectra were recorded in transmittance band mode in the wavelength range from 4000 cm-1 to 400 cm-1 [51].

3.7.1.2. Scanning Electron Microscopy (SEM) Analysis

SEM is a versatile advanced instrument which is largely employed to observe the surface phenomena of the materials. The sample was shot in a SEM using high energy electron, and the out coming electrons/X-rays were analyzed. These out coming electrons/X-rays gave information about topography, morphology, composition, orientation of grains, crystallographic information, etc. of a material. Surface of Moringa Olifera (MO), rGO, and reduced graphene oxide coated moringa olifera (rGO/MO). The samples were determined using a highly customizable scanning electron microscope (JSM-IT300LV, JEOL, USA) coupled with a port for analytical attachment of energy dispersive X-ray (EDX) spectrometry [52].

3.7.1.3. UV-Visible spectroscopy

Ultra violet and visible spectra were recorded from the synthesized MO, rGO, and rGO/MO adsorbents using Beckman Coulter DU730 LS UV/Vis Spectrophotometer.

3.7.1.4. X-ray Diffraction (XRD) Analysis

X-ray diffraction studies were performed under ambient condition on X-ray diffract meter (XRD-7000, Shimadzu) using Cu-Kα (λ = 1.5418 Å) radiation with 40 kV and 30 mA on rotation between 10^0 to 70^0 at 2θ scale. XRD analysis were used to examine the structure of MO, rGO and rGO/MO

3.7.1.5. Electrical Conductivity Studies

Electrical conductivity of MO, rGO and rGO/MO were measured using portable conduct meter device by dissolving in deionized chloroform solution.

3.7.2. Fe^{2+} determination procedures

UV-visible spectrometer was used to measure concentration of Fe^{2+} in treated water samples. Each samples were prepared and its absorbance was measured and used to get calibration curve for Fe^{2+} determination as follows.

1. The raw ground water was collected using polyethylene plastic holder from a source of the selected area, acidified and stored at 4°C refrigerator.
2. Then it was filtered and collected with less concentration of iron within three 250ml volumetric flasks.
3. 1 mL of 1M Sodium acetate ($C_2H_2NaO_2$), 1mL 10% Hydroxylamine HCl and 10mL of 0.3% ophenanthroline reagents were added to the three filtered water samples.
4. Then it was mixed thoroughly with distilled H_2O and dilute to a total volume of 50mL and allowed each solution to stand for at least 20 minutes at room temperature, to provide time for formation of the iron-phenanthroline complex.
5. Finally the Colorimetric Determination of ferrous iron was developed using UV-VIS and constructed calibration curve.

3.7.3. Adsorption procedures

1. The raw ground water was collected using polyethylene plastic holder from a source of the selected area, acidified and stored at 4°C refrigerator.
2. Then filtered water was collected with less concentration of iron.
3. 5, 10, 15 and 20 ppm of standard iron solution was prepared from 1000 ppm of iron solution by diluting with deionized water in 100 mL of volumetric flask.
4. Then, the variables would set up in order to identify the effect of adsorbent dosage, pH, initial concentration, as well as the effect on contact time of rGO/MO composite.

5. To study the effect of adsorbent dosage, pH, as well as the effect on contact time; different mass of adsorbents (0.02, 0.04, 0.06 and 0.08 g at different pH range (3.0-9.0) was mixed with contact time varies from 30 to 90 minutes.
6. All batch adsorption experiments were performed on a mechanical shaker with a shaking speed of 180 rpm.
7. After that the prepared and weighed MOSP and rGO composite coagulant was mixed with a 50 ml of raw and aqueous water.
8. Finally the treated water quality was further checked by UV-VIS spectroscopy.
9. A calibration curve of different concentrated solutions which were analyzed by UV-visible spectrophotometer also plotted.

4. RESULTS AND DISCUSSIONS

4.1. Physio-chemical analysis

Three shallow well ground water samples were collected from Wolicho,Araticho and Zigaz kebeles from Endegagn woreda and the physicochemical parameters like pH, turbidity, electric conductivity, total suspended solid (TSS), total dissolved solid (TDS), chloride, alkalinity and Hardness were measured as follows.

Table 2: The result of physico chemical parameter Values expressed as mean ± SD for triplicate.

Parameters	**Unit**	**Current Study (Sample site)**				**References**	
		Welicho	Araticho	Zgaze	95%Confidence limit	WHO [44,45,46]	EEPA [44,45,46]
-pH		7.02±0.1	6.7±0.17	7.11±0.1	6.96±0.19	6.5-8.5	6.5-8.5
Conductivity	**µs/cm**	113.3±0.5	77.5±0.7	150.6±0.9	113.8±25.9	1000	1500
Temperature	**°C**	21.8±0.4	22.4±0.15	22.6±0.08	22.3±0.37	≤ 40	40
Turbidity	**NTU**	21±1	16±1	24±1	20.3±2.93	5	5
TSS	**mg/L**	90±10	60±10	70±10	73.3±12.89	30	≤50
TDS	**mg/L**	95.2±0.35	79.8±0.6	121±0.38	98.7±14.69	500	1000
Total Alkalinity	**mg/L**	340±60	466±76.4	250±50	352±88.15	200	200
Total hardness	**mg/L**	150±30	150±36	250±30	183.3±45.05	300	-
Chloride		110±5	95±2.5	123.7±1.5	109.57±10.28	250	250
Fe	**mg/L**	0.65	0.66	0.62	-	0.3	0.3

The results of the study could be ranged as pH (6.52-–7.22), Temperature (21.3–22.7 oC), E.C (76.8–151.3 µS/cm), turbidity (15–22 NTU),TDS (79.2–121.3 mg/L), TSS (50–100 mg/L), hardness(120–280 mg/L), chlorides(93–125 mg/L), alkalinity (200–550 mg/L) and Fe^{2+}(0.62–0.66 mg/L). These insures that the values of most of the parameters such as pH, conductivity, temperature, TDS, hardness, and chloride content were within the permissible limit of WHO

and EEPA. However, the concentration of Fe^{2+} was above the maximum permissible limit set by WHO. Similarly, the values of physicochemical parameters such as turbidity, TSS, and alkalinity were above the acceptable range for drinking water limit set by WHO and EEPA. Thus, the result showed that the potable ground water collected from rural areas pose a risk to human health unless a proper water treatment system is implemented.

4.1.1. pH of water

The pH of pure water refers to the measure of hydrogen ions concentration in water. It ranges from 0 to 14. In general, water with a pH of 7 is considered neutral while lower of it referred acidic and a pH greater than 7 known as basic. It is noticed that water with low pH is tend to be toxic and with high degree of pH it is turned into bitter taste. It was very important parameter of water that would be measured because it influences the other physicochemical parameters and the availability of metal ion in the water. According to WHO standards pH of water should be 6.5 to 8.5. Hence all samples were within the range of the standard of WHO and EEPA there was no health effect regard to pH of the studied water sample [44].

4.1.2. Electrical Conductivity (EC)

Pure water is not a good conductor of electric current rather a good insulator. Increase in ions concentration enhances the electrical conductivity of water. Generally, the amount of dissolved solids in water determines the electrical conductivity. Electrical conductivity (EC) is actually measures the ionic process of a solution that enables it to transmit current. Conductance is not harmful but water with higher conductance is not suitable for irrigational and drinking purpose. According to WHO standards EC value should not exceeded 1000 µS/cm. The EC of the studied samples was 77.5, 113.3 and 150.6 µS/cm which was within the threshold limit. These results clearly indicated that water in the study area was not considerably ionized and had the lower level of ionic concentration activity due to small dissolve solids [44, 46].

4.1.3. Temperature

Temperature effects the seasonal and diurnal variation. It controls the rate of all biochemical and biological reactions including growth, multiplication, decay, mineralization, production etc. Temperature was recorded with the help of maximum minimum thermometer. All samples in the study area were less than permissible limit (40 ℃) which was set by WHO and EEPA [45].

4.1.4. Turbidity

Turbidity is a measure of cloudiness of water. It has no health effects. However, turbidity can interfere with disinfection and provide a medium for microbial growth. High turbidity may indicate the presence of disease causing organisms. These organisms include bacteria, viruses, and parasites that can cause symptoms such as nausea, cramps, diarrhea, and associated headaches (AKato and Adiyiah, 2007). In this study, all samples had turbidity value greater than 5 NTU, which was the WHO and EEPA maximum desirable limit in drinking water. These results indicated that, it might be due to the presence of colloidal and suspended matter (such as clay, silt, finely divided organic and inorganic matter, plankton, and other microscopic organisms). The added presence of turbidity increases the apparent, but not the true color of water.

4.1.5. Total Suspended Solid (TSS)

All samples had high TSS values range from 70 to 90 mg/L, However the permissible limits of TSS value stated by WHO was ≤ 30 mg/L. These might result high contamination of water and may introduce different diseases which affect all living things. Suspended solids are closely linked to nutrient transport (phosphor, especially), metal, industrial waste and chemicals used in agriculture transport.

4.1.6. Total Dissolved Solids (TDS)

Water has the ability to dissolve a wide range of inorganic and some organic minerals or salts such as potassium, calcium, sodium, bicarbonates, chlorides, magnesium, sulfates etc. These minerals produced un-wanted taste and diluted color in appearance of water. There is no agreement have been developed on negative or positive effects of water that exceeds the WHO standard limit of 1,000 ppm. Total dissolved solids (TDS) in drinking water is originates many ways from sewage to urban industrial wastewater etc. Therefore, TDS test was considered as a sign to determine the general quality of the water. The upper and lower total dissolved solid values of the sample were 79.8 $\pm$ 0.6 ppm and 121$\pm$ 0.38 ppm respectively. Therefore, health risks are not significant as the value of TDS was much less than WHO standard maximum permissible limit [44].

4.1.7. Total Alkalinity

The capacity of water to neutralize a strong acid is called alkalinity of water. Moderate concentration of alkalinity is desirable in most water supplies to stable the corrosive effects of acidity. However, excessive quantities may cause a number of problems. For drinking water, the maximum allowable concentration of total alkalinity is 200 mg/L according to both WHO and EEPA. In the absence of alternate water source, alkalinity up to 600 mg/l is acceptable. The alkalinity of the samples were slightly higher than permissible limit, might be due to carbonates and bicarbonates present in ground water. It was determined by simple dilute HCl titration in presence of methyl red indicator [45].

4.1.8. Chloride Contents

Chloride may present naturally in groundwater and may also originate from diverse sources such as weathering, leaching of sedimentary rocks and infiltration of Sea water etc. It was measured by titrating a 50 ml of sample with standardized silver nitrate solution using potassium chromate solution as an indicator. The samples had chloride values of 95,110 and 123.7 mg/L in ascending order which was lower than the maximum permissible limit of chloride in potable water stated by WHO (250 mg/l) [44]. High concentrations of Chloride could make water unpalatable and therefore, unfit for drinking or livestock watering.

4.1.9. Total hardness (TH)

In groundwater hardness is mainly contributed by bicarbonates, carbonates, sulphates and chlorides of calcium and magnesium. So, the principal hardness causing ions are calcium and magnesium. It was measured by titration method by standardized EDTA solution using Erichrome black T as indicator. Durfor and Becker (1964) have classified water as soft, moderate, hard and very hard [45]. It is the property of water that avoids the lather creation with soap and enhance the boiling point of water. Hard water is characterized with high mineral contents that are usually not harmful for humans. According to World Health Organization (WHO) hardness of water should be 300 mg/l. The samples had lower hardness than permissible limit [46].

4.2. Determination of ferrous iron (Fe^{2+}) concentration in ground water

The quantification of ferrous iron (Fe^{2+}) concentration in the three samples of the ground water was done by using UV-visible spectroscopy. The ligand utilized to form a colored complex was 1, 10-phenanthroline, or o-phenanthroline. Only Fe^{+2} reacted with o-phenanthroline and absorbed in the visible spectrum (around 510 nm). This reaction takes place under acidic conditions. Sodium acetate was used to buffer the solution that the complex will form in and hydroxylamine HCl was used to prevent oxidation. After making colorimetric measurements on various concentrations of solutions, a calibration curve was constructed. An unknown was analyzed for iron as well. [26]. Calibration curve was constructed for ferrous iron (Fe^{2+}) by plotting simultaneous metal ion concentration (5, 10, 15 and 20 ppm) versus their respective absorbance as shown in appendix part of this study.

Figure 5 above shows a linear function when absorbance is plotted versus the concentration of standards at 510nm (λmax) as predicted by Beer's Law. By using the calibration curve equation and the absorbance of the unknown sample treated under the same experimental conditions, the unknown concentration of sample can be calculated. The calibration curve equation y = 0.0026x + 2E-4 where "y" represents the absorbance at the given wavelength, "x" is the concentration of the unknown, "m" which is the slope of the line refers to the molar absorptivity, ε and "b" is the path length light has traveled to the sample. A regression of 0.9994 signifies that the reliability of the data points is linearly fit. From the calibration curve shown in figure 5 the concentration of the three unknowns was computed using the formula: $\mathbf{C_{unk} = (A_{unk} - y_{int.})/slope}$ by accounting for the dilution factor [26]. The final Fe^{2+} concentration determined and calculated from Beer-Lambert Law is summarized in the table below as follows.

Table 3: the final Fe^{2+} concentration determined for the three samples.

NO	Sample	Absorbance (A)	Absorptivity coefficient /slope/(ε)/ $M^{-1}cm^{-1}$	Path length (l)/y-intercept/	Concentration of Fe^{2+} calculated (C) /mg/L/
1	Zigeze(1)	1.617	0.0026	2.00E-04	0.62
2	Araticho(2)	1.715	0.0026	2.00E-04	0.66
3	Welecho(3)	1.692	0.0026	2.00E-04	0.65

As shown in table 4 above the concentration of Fe^{2+} of all samples were above the permissible level of iron in drinking water sated by WHO (0.3 g/ml). Therefore, it is imperative to remove this elevated amount of ferrous iron using 0.02g/L a new effective adsorbent (rGO/MO).

4.3. Characterization of prepared Adsorbents

4.3.1. Fourier Transforms Infrared (FT-IR) Spectroscopy

An FTIR spectrum is a useful tool commonly used to identify functional groups that are attached to a certain surface. It was used to analyze the chemical structure spectra of moringa oleifera (MO), reduced graphene oxide (rGO), and their new composite (rGO/MO) samples. The FTIR spectra were recorded in transmittance band mode in the wavelength range from 4000 cm^{-1} to 400 cm^{-1}[51].

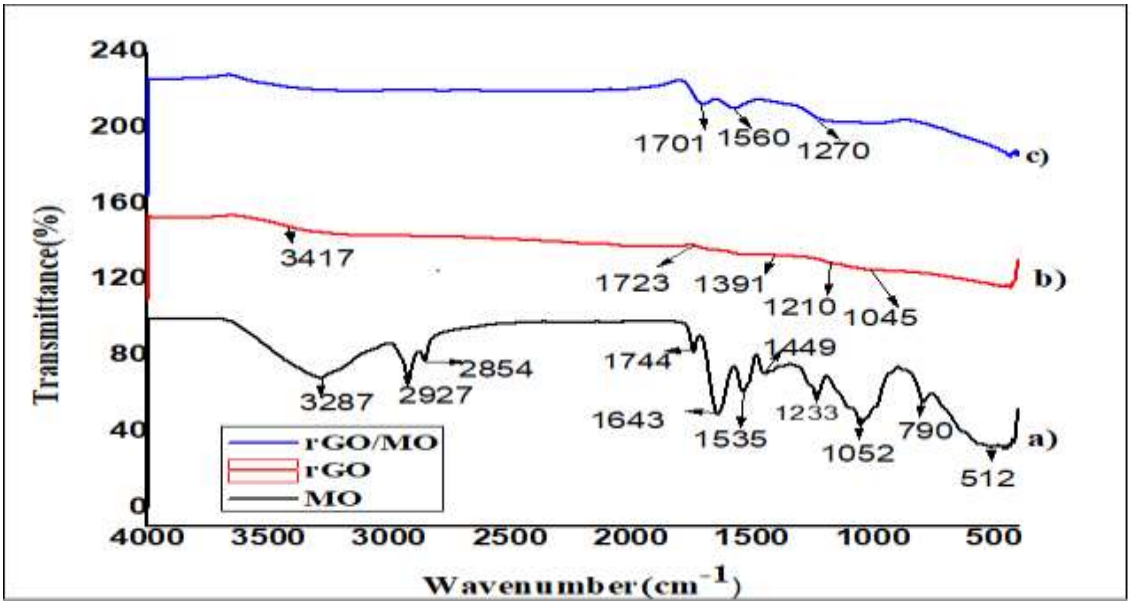

Figure 5: FT-IR spectra of a) MOSP b)rGO and c) rGO/MO

a) The FTIR spectra of MOSP (Figure 5a) above showed the presence of many functional groups, indicating the complex nature of the biosorbent. A strong peak at 3287 cm^{-1} indicates the presence of the hydroxyl group (-OH) stretching vibration (Kumar and Tamilarasan, 2013; Zhang et al., 2013; Sivaraj et al., 2001), which could belong to the proteins, fatty acids, carbohydrates and phenol compounds. A contribution in this region for the vibration stretching of the N–H bond of amide groups may be related to the protein content in the *moringa* seeds. The peak at 2927 and 2854 cm-1 indicates the presence of symmetric and asymmetric -C-H stretching bond of the CH_2 groups preset in fatty acids. The peak at 1744 cm^{-1} was primary amine group contained CO stretching. The carbonyl group was present in the fatty acid and protein structures. The peak at 1643 cm^{-1} was due to the carbonyl group (-C=O) that could belong to the primary or secondary Amide compounds (NH_2CO). The band at 1535 cm^{-1} corresponds to the -C=C of Aromatics compounds. In the region of 1449-1233 $cm^{-1,}$ there was a series of weak peaks that could correspond to the presence of carboxylic acids. The strongest band at 1052 cm^{-1} was attributed to the -C-O bond, as a prove of the presence of phenols compounds, carboxylic acids and also showed the lignocellulosic structure of the *moringa olifera* seed that provide adsorption sites for the metal ions. Finally, the weak bands between
790-512cm^{-1} could correspond to the -CH bond of aromatics compounds. The presence of this band confirmed the protein structure in the Moringa seeds [53].

b) After reduction of GO the characteristic absorption of oxygen containing groups were relatively weakened in the case of rGO. There was an obvious decrease in the intensities of OH stretching vibration (3417 cm^{-1}), C=O (1723 cm^{-1}), C- OH (1391 cm^{-1}) and C- O (1210 cm^{-1} and 1045 cm^{-1}) vibration peaks in rGO compared to those in GO, indicating that chemical reduction was an effective method to remove oxygen containing groups of GO. The presence of extensive OH peaks after reduction was due to the presence of adsorbed water molecules [54].When reducing graphene oxide to graphene, the functional groups disappeared. This was clearly reflected in the FTIR spectrum (Figure 6) for not having bands corresponding to any functional groups. The presence of oxygen containing functional groups, such as C=O and C–O, further confirmed that the graphite indeed was oxidized into GO and was consistent with the literature. The presence of C=C groups showed that even graphite oxidized into GO; in the main structure of the layer, graphite was still retained [55].

c) The peak intensity was weak in graphite and strong in rGO and rGO/MO, confirms the formation of rGO and the MOSP were played a role in terms of surface functionalization results the formation rGO and rGO /MO from graphite.In addition to these epoxy (C-O-C) vibrations were observed at 1560 cm^{-1}. It was not found in pure graphite sample, showed the oxidation processes done in the sample. The bending vibration of epoxy C-OH was observed at 1270 cm^{-1} and the peak intensity was increased after the reaction and treatment with MO. The intensity of the peaks in rGO and rGO/MO was much higher than the graphite peaks. These results indicated that rGO was obtained by reduction of graphite and it had undergone a reaction with *Moringa oleifera* seed powder and -NH_2, COOCH and -OH functional groups able to bind ferrous iron in adsorption process [56].

4.3.2. Scanning Electron Microscopy (SEM) Analysis

SEM is a versatile advanced instrument which is largely employed to observe the surface phenomena of the materials. The sample was shot in a SEM using high energy electron, and the out coming electrons/X-rays were analyzed. These out coming electrons/X-rays gave information about topography, morphology, composition, orientation of grains, crystallographic information, etc. of a material, Surface of *Moringa Olifera* (MO), rGO, and reduced graphene oxide coated moringa olifera (rGO/MO).The samples were determined using a highly customizable scanning electron microscope (JSM-IT300LV, JEOL, USA) coupled with a port for analytical attachment of energy dispersive X-ray (EDX) spectrometry [52].

a) MO b) rGO c) rGO/MO

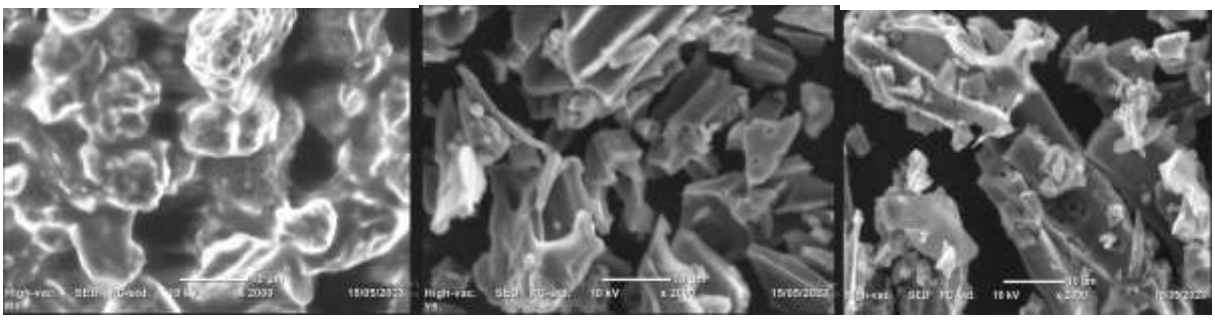

Figure 6: Scanning electron micrograph of a) MO, b) rGO, c) rGO/MO

a) *Moringa olifera* seeds have heterogeneous morphological characteristics, with high asymmetric porosity; it was a fibrous material, rich in cellulose and lignin. Due to its heterogeneous surface, the good adsorption capacity of this material was attributed to the pores

of the adsorbent surface; these available spaces facilitate the adsorptive process, as they provide a high internal surface of the material [31].It was also possible to concluded from the chemical characteristics of *Moringa olifera* seeds, that chemisorption phenomenon (ionic adsorption) can occur, due to the protein groups present in the adsorbent, and morphology of this material showed a heterogeneous and relatively porous matrix. This structure initiates the processes of ion adsorption, due to the interstices and, more importantly, to the presence of the protein component of the seed. Thus, based on these characteristics, MO has an adequate morphological profile for retaining graphene oxide

b) In general, the SEM image of the rGO was composed of platelets displaying a fluffy and crumpled morphology of a similar nature as that of the GO. These SEM images demonstrate thin and wrinkled platelets transparent to electrons in both cases [57].

c) SEM image of rGO/MO showed layers of sheets stacked over one another and are aggregated to some extent. The treated rGO's SEM image showed partial formation of rod structure which were again aggregated to some degree. Evidently, more number of wrinkles and foldings indicate greater reduction rate [56]. In rGO/MO, the wrinkles and folds have decreased when it's compared with MO and rGO. This confirms the interaction and chemical modifications occurred between the seed powder and reduced Graphene oxide.

4.3.3. UV-Visible spectroscopy

Ultra violet and visible spectra were recorded from the synthesized MO, rGO, and rGO/MO adsorbents using Beckman Coulter DU730 LS UV/Vis Spectrophotometer.

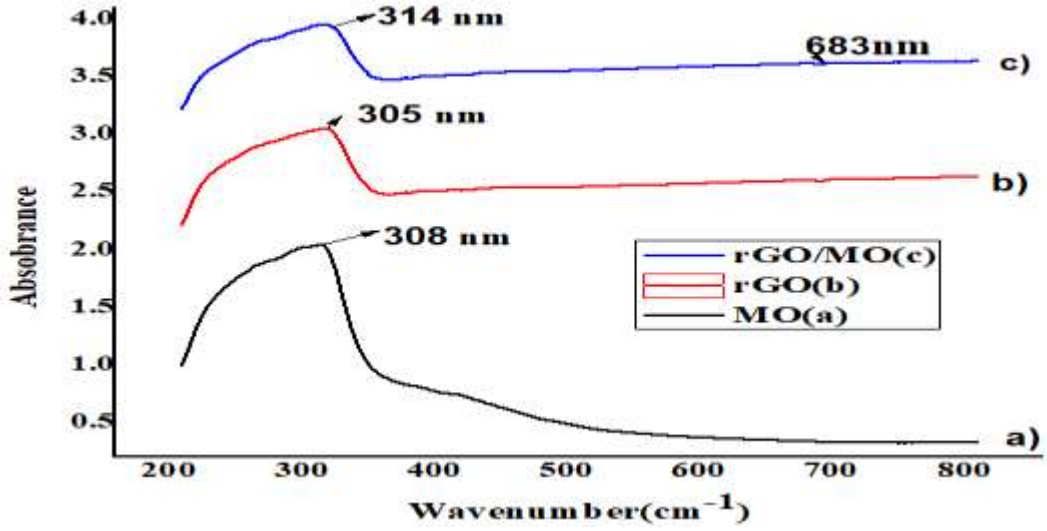

Figure 7: Ultra violet and visible spectra of a) MO, b) rGO, and c) rGO/MO

a) The absorption spectra of MO was due to π-π* transition from valance band to conduction band at 446 nm.

b) The absorption spectrum of the rGO sample demonstrated only a peak at about 270 nm, corresponding to the π→π* transition of the aromatic C–C bond. The peak at around 230 was red shifted to 270 nm after the reduction reaction, indicating that some groups on the GO surface were removed and the conjugated structure was restored in the final rGO structure. The reduction of GO to rGO was accompanied by the retrieval of the electronic conjugation of graphene sheets through the removal of oxygen-containing functional groups. This removed the absorption peak at 294 nm, leading to a red shift in the absorption peak of rGO from 230 to 270 nm [58].

Considering the Tauc's relation in Equation (1) below, the band gap of the thin films were obtained by plotting graphs of $\alpha h\nu^{1/2}$ versus hν and extrapolating the straight portion of the graph on hυ axis at αhυ= 0. The band gap has been calculated by absorbance co-efficient data as a function wave length using Tauc relation.

$(\alpha h\vartheta)=\beta[h\vartheta - Eg]^{n}$……1

where α is the absorbance coefficient, $h\vartheta$ is the photon energy, β is the band gap tailing parameter, *Eg* is a characteristics energy which is termed as β and *n* is the transition probability index with discrete value like 1/2, 3/2, 2 or more depending on transition of direct or indirect or forbidden band gap. The absorption coefficient (α) at corresponding wavelength was calculated by using Beer Lambert's relation [26].

$\alpha = \frac{2.303\ A}{l}$ … … … … … … … … … … … … … … … … … … …2

Where l is the path length and A is the absorbance

The plot $(\alpha h\vartheta)^{1/2}$let be D Vs hϑ (C) was linear function indicating the existence of direct allowed transition in MO, rGO, and rGO/MO. Extrapolation of linear dependence of the relation to yield corresponding band gap.

a) MO b) rGO c) rGO/MO

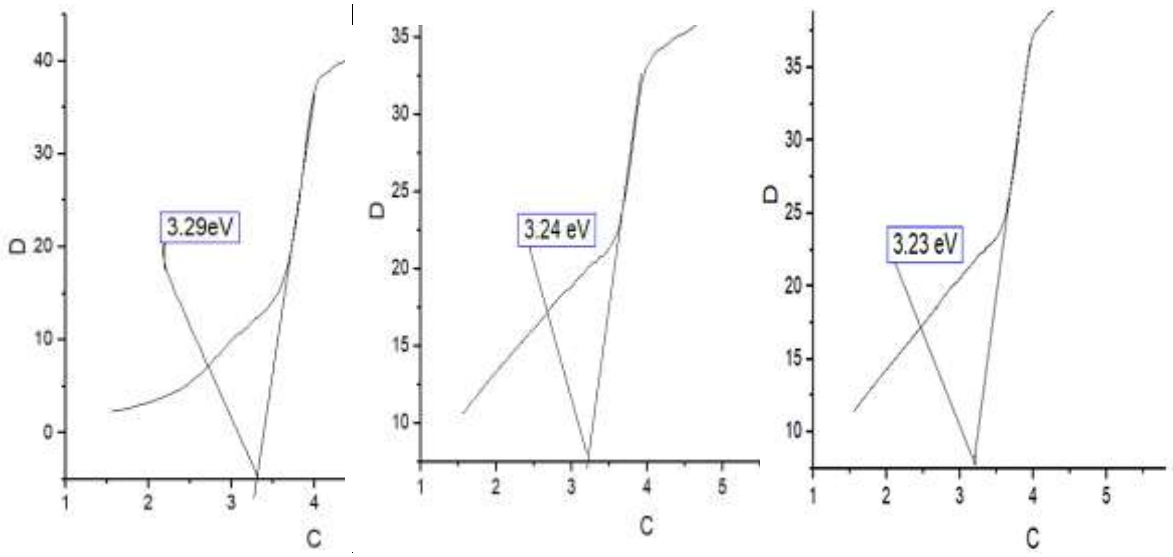

Figure 8: Linear plot $(\alpha h\vartheta)^{1/2}$ Vs $h\vartheta$ UV-visible band gap determination of the a) MO, b) rGO, and c) rGO/MO

The values of the optical band gap obtained in Fig 8a) MO, b) GO, and c) rGO/MO was calculated as 3.29, 3.24 and 3.23 eV respectively. The values of optical band gap were decrease from MO to rGO after deposition on surface of MO with acids implying decreases in conductivity. The reduction optical band gap of rGO/MO was due to the dimensions of resulting ions play an important role in the process of diffusion, it was known that acids are compounds that dissociate in water only to give positive hydrogen ions and negative ions of the acid residue, the disorder of the system, and surface modifications of the rGO on MO.

4.3.4. X-ray Diffraction (XRD) Analysis

X-ray diffraction studies were performed under ambient condition on X-ray diffract meter (XRD-7000, Shimadzu) using Cu-Kα (λ = 1.5418 Å) radiation with 40 kV and 30 mA on rotation between 10^0 to 90^0 at 2θ scale. XRD analysis were used to examine the structure of MO, rGO and rGO/MO

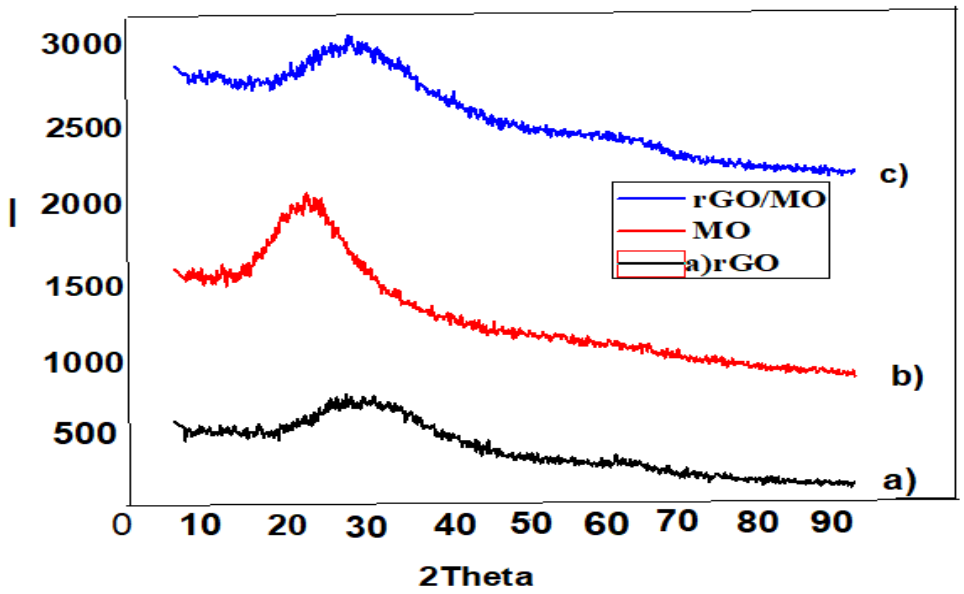

Figure 9: X-ray diffractograms of a) MO b) rGO c) rGO/MO

Fig.9a) shows the X-ray diffraction patterns of amorphous M. olifera seeds. Due to the high amount of proteins present in the composition of the material, around 69% by weight the X-ray pattern showed a poorly resolved peak that indicates a predominance of amorphous material. It was possible to separate a broad peak at 2θ = 10.8°. The presence of this peak was probably associated with diffraction of the constituent protein surrounding the other components that had a more amorphous nature.

b) According to the XRD results, the (002) plane of graphite with a d spacing of 0.38 nm was responsible for the sharp peak that was seen at 2θ = 26.3226. Notably, the graphene oxide peak (around 2θ = 10.52) did not form during the oxidation process; instead, a broad peak in the range of 24.3034 with a d-spacing of 0.36 nm was found. The development of residual oxygen functions in rGO sheets might be to blame for this. Peak broadening in the rGO was said to be related to the creation of layers or sheets, as was the difference in the d spacing values (0.01 nm). The suggested reaction method also facilitates the direct synthesis of rGO. Due to the rGO's residual O_2 and H content, the layer to layer distance was substantially greater than it was for graphite [56].

On the other hand, after reduction of GO, the 002 peak gradually disappeared, whereas the broad diffraction peak was observed in 2θ =24.96 (d = 6.0). This shift in the interlayer spacing was due to the reduction of the GO, where the reduction makes the rGO packing tighter than that of

GO due to the removal of most of oxygen atoms. In addition, the grain size was found to be 20.68 nm, as calculated by the Scherrer equation. $D = \frac{k\lambda}{\beta \cos\theta}$ ……(3) where: D is the mean size of the ordered crystalline, K is a dimensionless shape factor with a value of about 0.9 but varies with the actual shape of the crystallite, λ is the X-ray wavelength, β is the line broadening at half the maximum intensity (FWHM), and Θ is the Bragg angle [59].

From the XRD data, the crystal size of MO, rGO and rGO/MO was determined by using above from the 2.60nm, 6.0 nm, and 5.66 nm respectively.

Table 4: Average particle size of MO, rGO and rGO/MO samples

Sample	2Θ	Θ	Cos(Θ)	FWHM	β(FWHM$^{1/2}$	D(nm)
MO	10.88	5.44	0.67	12.81	3.58	2.60
rGO	1.9	0.95	0.58	2.26	1.5	6.0
rGO/MO	2.156	1.078	0.47	2.54	1.6	5.66

4.3.5. Electrical conductivity studies

The electrical conductivity of moringa olifera seed was 0.154 S/cm while that of rGO and rGO/MO were found 0.149 S/cm and 1.84 S/cm, respectively. The conductivity of rGO/MO was in the semi conducting level, which was clear evidence that rGO was deposited on MO. The deposition of rGO coated moringa olifera was rich in hemicellulose, lignin and other waxy substance confirmed from the FT-IR and XRD spectra. These impurities including the porous it restricted the movement of ions in the solution.

4.4. Bach experiments study

4.4.1. pH effect

The role of pH in adsorption is vital, as it affects surface functional groups of the adsorbent, the adsorbate species in solution, and ultimately adsorption capacity. The effect of pH on ferrous iron adsorption (Figure 11) showed that there was increase in percentage adsorption across the pH range 2−9.The percentage adsorption increases with pH to attain its maxima at pH of 9. The maximum removals of Fe^{2+} at pH of 9 were found to be 90%. With increase of pH from 2 to 9, the metal exists in the medium and surface protonation of adsorbent was minimum, leading to the enhancement of metal adsorption [60].

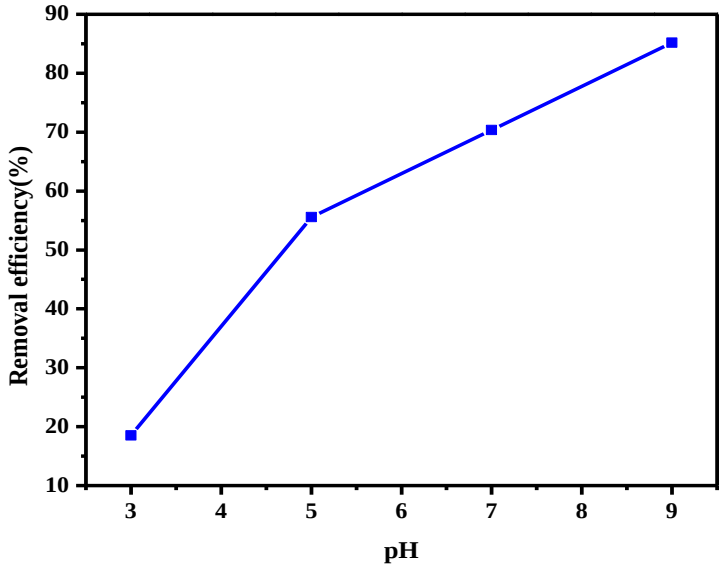

Figure 10: Effect of pH on removal Percentage of rGO/MO

4.4.2. Adsorbent dosage effect

According to alias et. al., (2012), the adsorption capacity decreases as the adsorbent dose increases. This is due to the fact that at higher adsorbent dosage, the solution metal ion concentration drops to a lower value and the system reaches equilibrium at lower values indicating the adsorption sites remain unsaturated. Hence further increase in the mass will not bring about appreciable adsorption because almost all the metal ions might have been removed. In addition, Kumar et al., (2010) also concluded that this reducing trend is because as the adsorbent dose increases, the number of adsorbent particles increases and thus more iron is attached to their surfaces and the adsorption sites remain unsaturated. Similarly in our experimental studies the adsorption of Fe^{2+} were decreased as the dose of rGO/MO composite increases. The maximum removal efficiency was found at 0.02g of the rGO/MO composite as shown in figure [52].

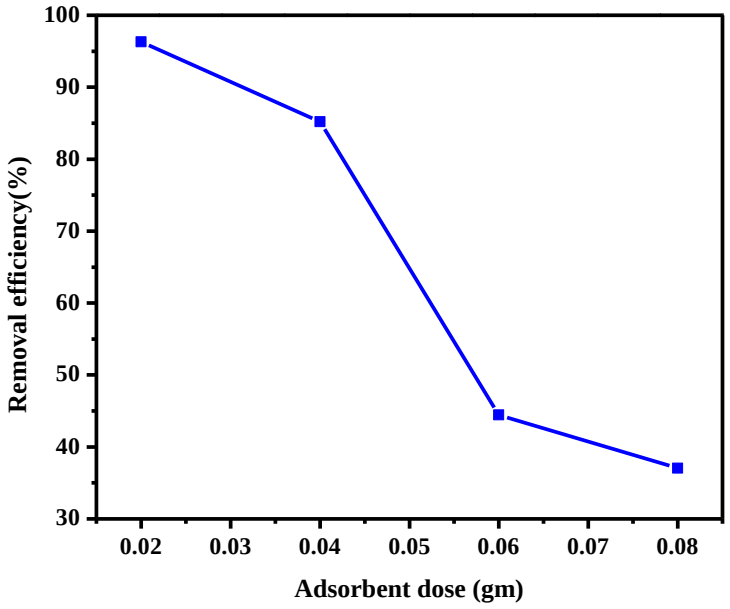

Figure 11: Adsorbent dosage effect on removal efficiency of rGO/MO

4.4.3. The effect of contact time

According to O. Akpotu Samson et al, studied in wastewater treatment, rapid removal of pollutants is essential. The optimal contact time for rGO/MO adsorbent to adsorb Fe^{2+} occurred at 50 min as showed in Figure 13 below. Initially, there was rapid adsorption of the adsorbate molecules because of vacant sorption sites on the adsorbents, followed by a slow pace leveling off after sorption sites became occupied. Such extremely rapid kinetics were attributed to mesoporosity and functional groups from the rGO/MO molecules [60].

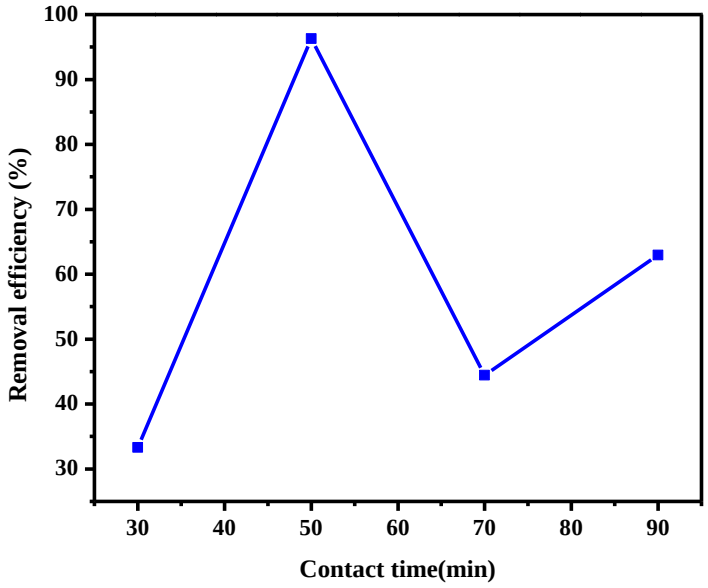

Figure 12: Effect of contact time on removal efficiency of rGO/MO

4.4.4. Effect of initial concentration of Fe^{2+}

According to Nohier El-Bendary et al, studied the removal efficiency of adsorbent decrease, when the initial Fe (III) concentration increases from 5 to 40 mg/L. This is may be due to the aggregation of iron ions at higher concentrations to large sized micelles which are difficult to diffuse through the microspores of the adsorbents [61]. At lower initial metal ion concentrations, sufficient adsorption sites are available for adsorption of the heavy metals ions. However, at high concentration the available sites of adsorption become fewer [10]. Our study was fit with this literature as shown from fig.13 below. The effect of initial Fe^{2+} concentration on the adsorption rate was studied in the rage (5 to 20mg/L) at pH 9, adsorbent dose 0.02g, and contact time of 50 min. Therefore, it was evident from the results that Fe^{2+} adsorption was dependent on the initial metal concentration.

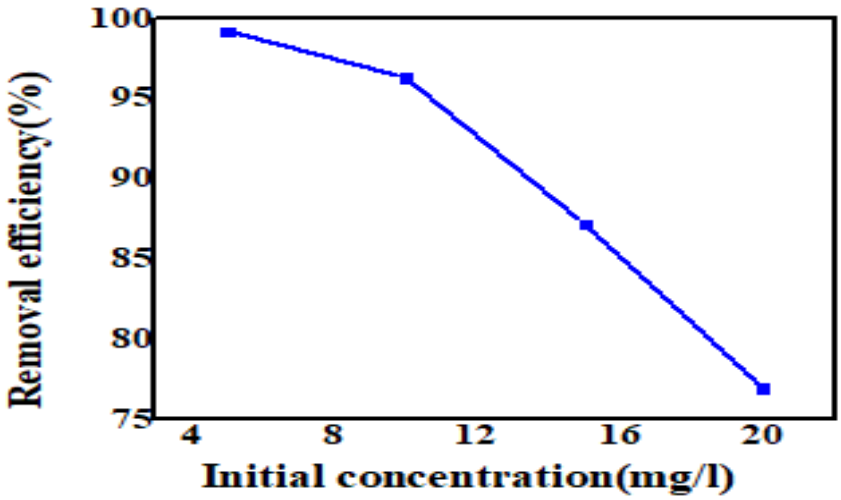

Figure 13: Initial concentration effect on removal efficiency of rGO/MO

4.5. Adsorption Study

The batch adsorption study was used to access the adsorption capacity of adsorbent. The amount of metal ion adsorbed onto rGO/MO adsorbent was determined by using following equation.

$Q_t = (C_i - C_e/W) \times V$……..... (4)

Where, Ci = Initial concentration of metal ion (mg/L), W = Weight of adsorbent (g).

Ce = Equilibrium concentration of metal ion (mg/L). Qt = Amount of metal ion adsorbed onto adsorbent at time‘t’ (mg/g), V = Volume of metal ion solution (L)

Likewise metal ion removal percentage was calculated by using the following equation.

$R\% = (C_i - C_e/C_i) \times 100$…….. (5) [40].

According to Khati Varada and Gulwade Deepali, the pH dependence study of the adsorption process revealed that maximum Iron removal using activated carbon of moringa olifera seed pod husk was 88.73% [20]. In this study the highest removal efficiency of rGO/MO was observed 99% for Fe^{2+} ions at pH of 9.0 this indicates the effectiveness of the new composite adsorbent (rGO/MO) to remove Fe (II) in ground water.

4.5.1. Langmuir Adsorption Isotherm

Is given by; qe = qm ka Ce / (1+ ka Ce)…….... (6)

Where: qe: The amount of iron adsorbed per unit mass at equilibrium (mg/g)

qm: The maximum possible amount of iron that can be adsorbed par unit mass of adsorbent (mg/g) Ce: Concentration of adsorbate in the solution at equilibrium (mg/l) Ka: equilibrium constant

The linearized form of equation (9) is: Ce / qe = 1/ (Ka qm) + Ce / qm ..... (7)

The essential characteristics of Langmuir isotherm can be expressed in the terms of dimension less separation factor RL, which is defined as: RL = 1/ (1+ Ka Co)..... (8)

Where: RL: Dimension less separation factor Ka: Langmuir constant Co: The initial concentration of iron (mg/l) [42].

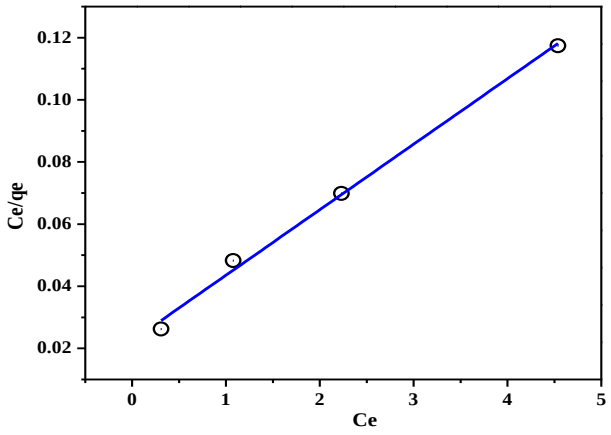

Figure 14: Langmuir isotherm (Ce/qe vs Ce for the adsorption of Fe2+ on rGO/MO

Table 5: Langmuir isotherm model of synthesized rGO/MO adsorbent

Langmuir isotherm model	synthesized samples
	rGO/MO
q_{max} (mg/g)	44.64
R_L	0.15
K_L (L/mg)	1.06
R^2	0.994

The relation between the initial concentration of Fe^{2+} and its percentage removal from solution was studied for anew innovative rGO/MO adsorbent prepared in this study. The initial concentrations of Fe^{2+} studied was 5 mg/L at an adsorbent concentration of 0.02g/L. The adsorption equilibrium data are conveniently represented by adsorption isotherms, which correspond to the relationship between the mass of the solute adsorbed per unit mass of adsorbent qe and the solute concentration for the solution at equilibrium C_e. Linear plots of C_e/q_e versus Ce (Fig. 14) were employed to determine the value of q_{max} (mg/g) and KL (L/mg). The highest value of adsorption capacity q_{max} (maximum uptake) was 44.64 mg/g. According to McKay et al. RL values between 0 and 1 indicate favorable adsorption[35]. In our case the RL value for the adsorption of Fe^{2+} on rGO/MO adsorbent was within this range, so rGO/MO is a good adsorbent for adsorption of elevated Fe^{2+} ion from ground water.

4.5.2. Freundlich Adsorption Isotherm

Freundlich adsorption isotherm model is a type of isotherm model in which the absorbents form a monomolecular layer on the surface of the absorbent, but unlike the Langmuir model, application to multilayer adsorption is also possible. The Freundlich model expression shows the heterogeneity of the surface of the molecules as well as the exponential distribution of active sites and their energies.

The non-linearized form of Freundlich isotherm model expression the linearized form is shown in Equation $Qe = KFCe^{1/n}$

ln Qe = ln KF + 1n ln Ce (12) where KF is the Freundlich constant or maximum absorption capacity (L/mg), n is the adsorption intensity or surface heterogeneity, which indicates the energy distribution and the absorbate site's heterogeneity [43].

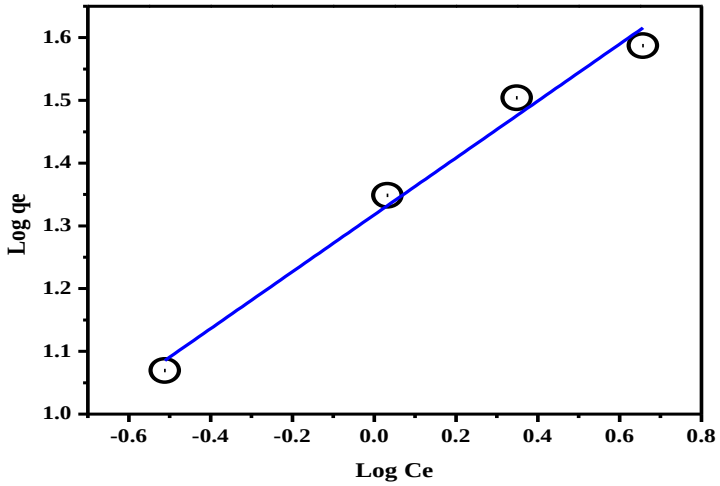

Figure 15: Freundlich isotherm (log qe Vs log ce) for the adsorption of Fe2+ on rGO/MO

Table 6: Freundlich isotherm model of synthesized rGO/MO adsorbent

Freundlich isotherm model	synthesized samples
	rGO/MO
K_F (mg/g)	20.78
(n)	2.20
1/n	0.45
R^2	0.979

The equilibrium data also fitted to Freundlich equation (Eq. (4)), a fairly satisfactory empirical isotherm can be used for non-ideal adsorption. According to Bhatt, and A. S. Sakaria, if a value of n= 1, the adsorption is linear, for n< 1, the adsorption is chemisorption, and for n > 1 the adsorption is a favorable physical adsorption. Thus, analyzing the n values > 1 for adsorption of elevated Fe^{2+} ions onto rGO/MO was much favored the physical adsorption. The adsorption capacity Kf was highest for clarified sludge followed by rGO/MO.

4.6. Real sample adsorption study

The adsorption efficiency of rGO/MO composite adsorbent for Fe (II) at optimized initial concentration adsorbent dosage, pH and contact time was as follows:

Table 7: real sample adsorption data

Real sample removal efficiency			
Real sample	ab1	ab2	Rem.Eff.(%)
1	1.617	0.305	81.13790971
2	1.715	0.632	63.14868805
3	1.692	0.486	71.27659574

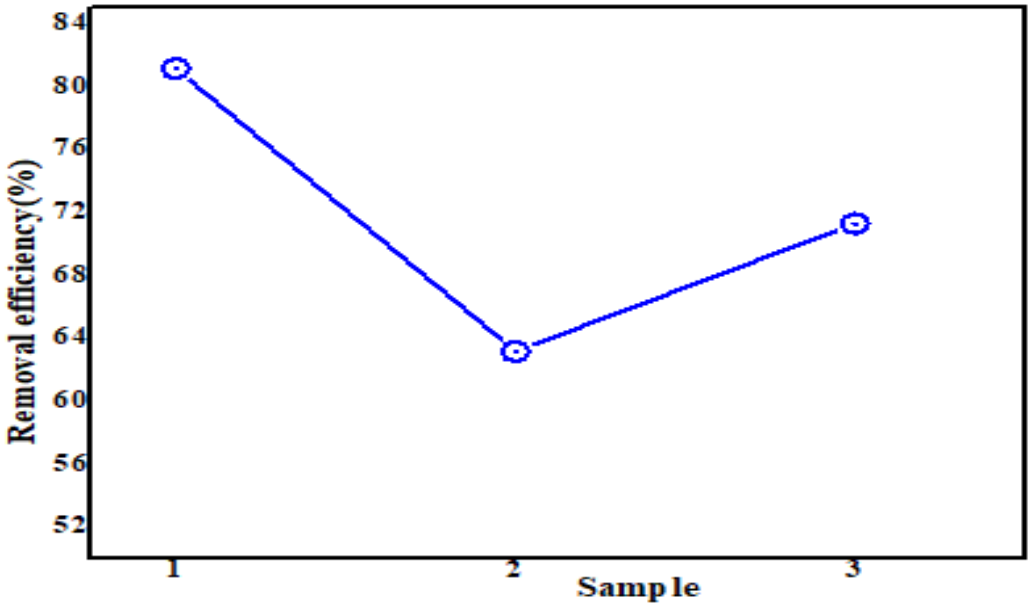

Figure 16: Removal efficiency of the real samples adsorption

As shown in the figure 16 above the adsorption efficiency of rGO/MO composite adsorbent for Fe (II) in the real samples at 5mg/g initial concentration, 0.02g adsorbent dosage, 9.0 pH and 50minute contact time were 81.1%, 63.1% and 71.2% in the sample1,2,3 respectively.

5. CONCLUSION AND RECOMANDATION

5.1. CONCLUSION

From this work, an effective adsorbents of MO, rGO and their composite (rGO/MO) were synthesized from Moringa olifera seed powder and reduced graphene oxide. GO was synthesized by using the Hummer method with little modification and reduced chemically using ascorbic acid. This was due to that chemical reduction is easy, low-cost, and has a high throughput and ascorbic acid was preferred because of its scalable production of rGO and did not produce toxic gases. Essential Analytical techniques such as (FTIR, SEM, UV and XRD) have been used to characterize the three synthesized adsorbents. Based on the results obtained this composites adsorbent were showed that a significant removal of ferrous iron from the water samples. The percentage removal of Fe (II) from ground water using rGO/MO strongly depends upon various parameters such as initial concentration, adsorbent dosage, pH, and contact time. The maximum adsorption capacity q_{max} of rGO/MO was (44.64 mg/g) at 5mg/g initial concentration, 0.02g adsorbent dosage, 9.0 pH and 50minute contact time. Experimental data were better fitted for Langmuir isotherm model (R^2 =0.994) than Freundlich adsorption isotherm model (R^2 =0.979). The adsorption efficiency of rGO/MO nanocomposite was 99.2% and 81.1%, from simulated and real dirking water samples respectively, when adsorbent dosage, pH, contact time, and intial concentration of iron were optimized. Therefore rGO/MO is an excellent adsorbent for Fe (II) removal from both simulated and real ground water samples.

5.2. RECOMANDATION

Based on the results and considerations in this study, there are a number of promising findings. However, the following issues are either given shallow attention or presented incompletely, and they are proposed for future work

- Further study could be conducted on other Physio-chemical and biological parameters on drinking ground water specifically in Endegagn Woreda and Gurage zone as a whole.
- Determination of heavy metal contaminants of drinking water other than iron which could affect human health such as zinc, lead, chromium, mercury, cadmium could be conducted.
- By widening the scope of the study further to see the adsorption studies like kinetic and thermodynamic studies of iron removal which are not included.
- In order to gain various benefit of an effective composite adsorbent (rGO/MO) further study like anti-microbial activity will be needed.

6. REFERENCES

1. Belay Lemlem. "Removal of iron and manganese from groundwater by oxidation-filtration hybrid system." *Master's thesis*, no. 3 (2020): 255-264.

2. Zaimee, M.Z.A.; Sarjadi, M.S.; Rahman, M.L. "Heavy metals removal from water by efficient adsorbents." *Water* 13, no. 19 (2021): 2659.

3. Gebrerufael, Hailu Kahsay et.al "Evaluation of groundwater quality and suitability for irrigation and drinking purposes Using Hydro chemical Approach: The Case of Raya Valley, Northern Ethiopia". *Momona Ethiopian Journal of Science (MEJS*), V11 (1) (2019):70-89.

4. Ranjit, N. Patil, et al. "A review on removal of iron in ground water by using low coast adsorbents." *IJARIIE-ISSN* 3(2017):2395-4396

5. Thakuria, Dipankar and Buddharatna J. Godboley. "Contamination and removal of iron and flouride from groundwater by adsorption and filtration: A review." *International Journal of Science Technology & Engineering 2*, no. 7 (2016): 80-85.

6. Khan, Masood Akhtar, et.al "Removal of iron from aqueous solution by using South Ethiopian Semen Ari Bamboo activated carbon." *International Journal of Scientific and Technology Research*, no. 9 (2020): 2277-8616.

7. Jubna, Jaber et.al "Adsorptive removal of lead and chromate ions from water by using iron-doped granular activated carbon obtained from coconut shells." *Sustainability* 14, no. 17 (2022): 10877.

8. Desai, B., and H. Desai. "Potential of *Moringa oleifera* (drum sticks) seeds and its application as natural adsorbent in removal of heavy metal ions." *International Journal of Environment, Ecology, Family and Urban Studies (IJEEFUS), ISSN* 3, no.4 (2013): 2250-0065.

9. Ravikumar, K., and A. K. Sheeja. "Heavy metal removal from water using *Moringa oleifera* seed coagulant and double filtration."*International Journal of Scientific & Engineering Research,* 9 (2013): 2229-5518.

10. Balaji, R., S. Sasikala, and G. Muthuraman. "Removal of Iron from drinking/ground water by using agricultural Waste as Natural adsorbents." *International Journal of Engineering and Innovative Technology* 3, no. 12 (2014): 43-46.

11. Azad, Md Shahin et.al "Efficiently Removal of Copper and Cadmium from Wastewater using Activated Carbon Produced from *Moringa oleifera* Bark". *International Journal of Engineering Research & Technology (IJERT)* 9, no.11 (2020): 2278-0181

12. Politaeva, et.al "Graphene oxide-chitosan composites for water treatment from copper cations." *Water* 14, no. 9 (2022): 1430.

13. Desissa, Daba. "Quality assessment of rural drinking water supply schemes from source to point of use. A case study of a Woreda, in Oromia Regional State of Ethiopia). *A Report to School of gradulate studies Addis Ababa instituite of technolgy* (2016).

14. Asfaw, Melese Damtew. "Assessment of Ground Water Quality in Woreillu town, Ethiopia." (2022).

15- Sankhla, Mahipal Singh, and Rajeev Kumar. "Contaminant of heavy metals in groundwater & its toxic effects on human health & environment." *Available at SSRN* 3490718 (2019).

16. Sihabudeen M. Mohamed, A. Abbas Ali, and A. Zahir Hussain. "Removal of heavy metals from ground water using *eucalyptus* carbon as adsorbent." *International Journal of ChemTech Research 9*, no. 03 (2016): 254-257.

17. Anake, Winifred U. et.al "Assessment of trace metals in drinking water and groundwater sources in Ota, Nigeria." *International Journal of Scientific and Research Publications 4*, no. 5 (2014): 1-4.

18. Clark, Jim Chemistry of iron..*Libere Textes* (2020).

19. Khati, Varada V. and Gulwade Deepali P. "Adsorption studies of Iron Removal from Aqueous Solution Using *Moringa Oleifera* Seed Pod Husk Activated Carbon as an Adsorbent."*Int. Res. Journal of Science & Engineering*, February 2020, Special Issue A7: 101-109.

20. Ahmad, Mansoor. "Iron and Manganese removal from groundwater: Geochemical modeling of the Vyredox method." *Master's thesis*, 2012.

21. Ankrah, Daniel Anobaah. "Elimination of iron from groundwater for drinking water purpose, and strategic transfer of the technology to developing countries such as Ghana." *Ph.D. Thesis Luma Print, 6700 Esbjerg*. (2012).

22. Lee, Sumin et al. "Iron detection and remediation with a functionalized porous polymer applied to environmental water samples." *Chemical science 10*, no. 27 (2019): 6651-6660.

23. Joseph, Mutula Joseph " Iron remova from boreholel: A case study of Town, Kiambu " *PhD diss., university of Nairobi,* 2016.

24. Adebayo, Basheer K, Hussein K. Okoro,"Spectrophotometric determination of iron (III) in tap water using 8-hydoxyquinoline as a chromogenic reagent." *African Journal of Biotechnology 10,* no. 71 (2011): 16051-16057.

25. Aregahegn, Meseret."Determination and Removal of Hexavalent Chromium. *"Master's thesis,* 9(2021): 2320-9151

26. Barry, Justin. "Inorganic Chemistry Dr. Berry Colorimetric Determination of Iron."

27. Ruiti, Manel, and Béchir Ben Thayer. "Removal of iron from artificial groundwater by adsorption on charcoal." *International Journal of Scientific Research & Engineering Technology (IJSET) ISSN* (2015): 2356-5608.

28. Heraldy, E., Y. Hidayat, and M. Firdaus. "The langmuir isotherm adsorption equation: the monolayer approach." *In IOP Conference Series: Materials science and engineering*, vol. 107, no. 1, p. 012067. IOP Publishing, 2016.

29. Alaqarbeh, Marwa. "Adsorption phenomena: definition, mechanisms, and adsorption types: short review." *RHAZES: Green and Applied Chemistry* 13 (2021): 43-51.

30. Binyam Kebede. "Assesment of Cactus potential as a Natural Coagulant in Water Treatment" *Master's thesis*, (2013): 31-32.

31. Makoona Zubairi "Effectiveness of *Moringa oleifera* coagulant in treatment of drinking water. "*A project report* (2017).

32. Jadhav Vikram et.al "Role of *Moringa oleifera* on green synthesis of metal/metal oxide nanomaterials." *Journal of Nanomaterials* (2022): 1-10.

33. Loryuenyong, Vorrada, Achanai Buasri. "Preparation and characterization of reduced graphene oxide sheets via water-based exfoliation and reduction methods*." Advances in Materials Science and Engineering* Volume 2013, Article ID 923403, 5 pages.

34. Köhler, Mateus H, et.al "Three-Dimensional and Lamellar Graphene Oxide Membranes for Water Purification." *In Two-Dimensional (2D) Nanomaterials in Separation Science, Cham: Springer International Publishing 8,* (2021): pp. 87-111.

35. Ray, Sekhar C. "Application and uses of graphene oxide and reduced graphene oxide." *nanomaterials 6,* no. 8 (2015): 39-55.

36. Ibrahim, Omar, Savaş Erdem, and Ezgi Gurbuz. "Studying Physical and Chemical Properties of Graphene Oxide and Reduced Graphene Oxide and Their Applications in Sustainable Building Materials." *In Advancements in Sustainable Architecture and Energy Efficiency, IGI Global* 10, (2021): pp. 221-238.

37. Xu, Jing, Hongda Lv, Sheng-Tao Yang, and Jianbin Luo. "Preparation of graphene adsorbents and their applications in water purification*." Reviews in Inorganic Chemistry 33*, no. 2-3 (2013): 139-160.

38. Mhemeed, Amal H. "A general overview on the adsorption." *Indian Journal of Natural Sciences 9,* no. 51 (2018): 16127-16131.

39. Sazali, Norsuhailizah, Zawati Harun, and Norazlianie Sazali. "A review on batch and column adsorption of various adsorbent towards the removal of heavy metal." *Journal of Advanced Research in Fluid Mechanics and Thermal Sciences 67,* no. 2 (2020): 66-88.

40. Shrestha, Sunita, Anita Kumari Dhami, and Armila Rajbhandari Nyachhyon. "Adsorptive Removal of Fe (II) By NaOH Treated Rice Husk: Adsorption Equilibrium And Kinetics." *Scientific World 14,* no. 14 (2021): 75-82.

41. Foo, Keng Yuen, and Bassim H. Hameed. "Insights into the modeling of adsorption isotherm systems." *Chemical engineering journal 156*, no. 1 (2010): 2-10.

42. Ruiti, Manel, and Béchir Ben Thayer. "Removal of iron from artificial groundwater by adsorption on charcoal." *International Journal of Scientific Research & Engineering Technology (IJSET) ISSN 3, no.2* (2015): 2356-5608.

43. Ehiomogue, Precious and Israel I. Ahuchaogu, "Review of adsorption isotherms models*." Acta Technica Corviniensis-Bulletin of Engineering 14*, no. 4 (2021).

44. Mohsin, Muhamed et.al "Assessment of drinking water quality and its impact on residents' health in Bahawalpur City." *International Journal of Humanities and Social Science 3*, no. 15 (2013): 114-128.

45. Varsha, Nigam and M.C. Kanchan"Physico-chemical parameters for testing of water-A review." *International Journal of Chemical Studies 3*, no. 4 (2015): 24-28.

46. Esubalew, Wubie "Physiochemical analyses on assessment to ground water quality parameters and ground water management options" *Master's thesis*, (2021): 20-21.

47. Mamo, Bekele Yirga, and Tegene Desalegn Zeleke. "Green synthesis of rGO/Ag nanocomposite using extracts of Cinnamomum verum plant bark: Characterization and evaluation of its application for Methylene blue dye removal from aqueous solutions." *International Journal of Nano Dimension 13*, no. 4 (2022): 414-434.

48. Razaq, Aamir et.al "Review on graphene-, graphene oxide-, reduced graphene oxide-based flexible composites: From fabrication to applications." *Materials 15*, no. 3 (2022): 1012.

49. Garje, Medha Gijare et.al "A study on characteristics of ecofriendly synthesis of graphene oxide using citrus limeta and l-ascorbic acid. *"Journal of Emerging Technologies and Innovative Research (JETIR)* 6, no.5 (2019): 2349-5162.

50. Alias, Nurul Zawani et.al "Removal of iron (Fe) by adsorption using activated carbon moringa oleifera (ACMO) in aqueous solution." *Jurnal Intelek 7*, no. 2 (2012): 22-29.

51. Amuanyena, Marta Ombili Ndakola. "Magnetic nanoparticles modified with Moringa seed proteins for water treatment and recovery of precious metal ions." *PhD diss., University of Namibia,* (2019).

52. K. Akhtar et al "Scanning Electron Microscopy: Principle and Applications in Nanomaterials Characterization." *Nanomaterials 10, no.3* (2019): 113-114.

53. Meneghel, Ana Paula et.al "Biosorption and removal of chromium from water by using moringa seed cake (Moringa oleifera Lam.)." *Química Nova 36 (2013): 1104-1110.*

54. Aragaw, Belete Asefa, and Atsedemariam Dagnaw. "Copper/reduced graphene oxide nanocomposite for high performance photocatalytic methylene blue dye degradation." *Ethiopian Journal of Science and Technology 12*, no. 2 (2019): 125-137.

55. Habte, Adere Tarekegne, and Delele Worku Ayele. "Synthesis and characterization of reduced graphene oxide (rGO) started from graphene oxide (GO) using the tour method with different parameters." *Advances in Materials Science and Engineering Volume 2019, Article ID 5058163, 9 pages* (2019).

56. M.Rajan et al."One Step Synthesis of Reduced and Moringa oleifera Treated Graphene Oxide: Characterization and Antibacterial Studies". *(Eds.): ICON, SPM,* (2019) pp. 54–62,

57. Fekade, Leouleseged Garedew. "Green reduction of graphene oxide using an extract from the leaves of moringa stenopetala." *PhD diss*., 2019.

58. Belay, Wasie. "Synthesis of Silver-Copper Reduced Graphene Oxide Nanocomposite and Its Catalytic Dye Degradation Activity." *PhD diss.,* 2022.

59. Hessain, Hayder A., and J. J. Hassan. "Green synthesis of reduced graphene oxide using ascorbic acid." *Iraqi Journal of Science* (2020): 1313-1319.

60. Akpotu, Samson O., Isiaka A. Lawal, Paul N. Diagboya, Fanyana M. Mtunzi, and Augustine E. Ofomaja. "Engineered geomedia kaolin clay-reduced graphene oxide–polymer composite for the remediation of olaquindox from water." *ACS omega 7*, no. 38 (2022): 34054-34065.

61. El-Bendary, Nohier, Hisham Kh El-Etriby, and Hani Mahanna. "High performance removal of iron from aqueous solution using modified activated carbon prepared from corn cobs and luffa sponge." *Desalin Water Treat 213* (2021): 348-357.

7. APPENDIX

7.1. Appendix A

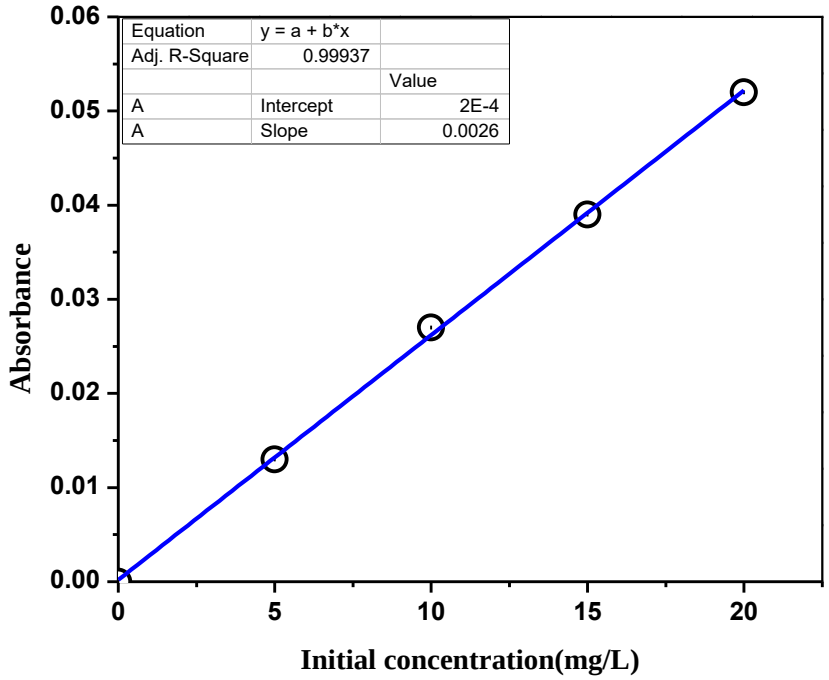

Figure: Calibration curve of standards

7.2. Appendix B

Languimer and Freundulich isotherm model				For rGO/MO			
I.conc	Ab1(Ci)	(Ce)	1/ce	Qe	ce/qe	logce	log qe
5	0.001	0.307692308	3.25	11.73076923	0.026229508	-0.5118834	1.069326491
10	0.003	1.076923077	0.928571429	22.30769231	0.048275862	0.03218468	1.348454646
15	0.006	2.230769231	0.448275862	31.92307692	0.069879518	0.34845465	1.504104744
20	0.012	4.538461538	0.220338983	38.65384615	0.117412935	0.65690866	1.587192714

Frendulich graphe adsorption experiment						
frendulich graphe log ce Vs log qe				Log qe=log Kf +1/n Log Ce		
			slope=1/n	Intercept =Log Kf		
				Kf=(antilog result of intercept value)		
Intercept	Slope	1/n	Kf	R^2	N	
1.31766	0.45359	0.45359	20.780692	0.97942	2.20463414	

7.3. Appendix C

A.D at PH 9				
A,D	Ab1	Ab2	RenEff%	Ce (M)
0.02	0.027	0.001	96.2962963	0.384615385
0.04	0.027	0.004	85.18518519	1.538461538
0.06	0.027	0.015	44.44444444	5.769230769
0.08	0.027	0.017	37.03703704	6.538461538
Initian C	Ab1	Ab2	Rem Eff%	Ce(M)
5	0.013	0.0001	99.230769	0.03846154
10	0.027	0.001	96.296296	0.38461538
15	0.039	0.005	87.179487	1.92307692
20	0.052	0.012	76.923077	4.61538462

Real sample removal efficiency			
Real sample	ab1	ab2	RemEff%
1	1.617	0.305	81.13790971
2	1.715	0.632	63.14868805
3	1.692	0.486	71.27659574

7.4. Appendix D

One-Way ANOVA						
		Sum of Squares	Df	Mean Square	F	Sig.
pH	Between Groups	.873	2	.364	1496.965	.001
	Within Groups	.001	9	.002		
	Total	.784	11			
EC	Between Groups	28687.2	2	8985.44	1261.808	.000
	Within Groups	7.808	9	.938		
	Total	26692.889	11			
TUR	Between Groups	32.553	2	8.28	34.900	.0001
	Within Groups	5.21	9	.621		
	Total	25.729	11			
TSS	Between Groups	1792.829	2	673.910	569.874	.000
	Within Groups	9.833	9	1.23		
	Total	1802.673	11			
TDS	Between Groups	11639.880	2	3546.330	7954.385	.000
	Within Groups	4.567	9	.446		
	Total	10642.557	11			
TA	Between Groups	161619.000	3	64873.000	190.120	.0001
	Within Groups	2278.667	9	374.833		
	Total	174897.677	11			

TH	Between Groups	274717.333	2	92582.434	543.154	.000
	Within Groups	1687.333	9	220.917		
	Total	287403.677	11			
Temp	Between Groups	.088	2	.040	1.550	.201
	Within Groups	.167	9	.031		
	Total	.357	11			
Cl	Between Groups	7157.323	2	3049.508	165.776	.000
	Within Groups	103.260	9	12.908		
	Total	6251.483	11			
Fe	Between Groups	5.252	2	1.514	10.041	.005
	Within Groups	1.167	9	.141		
	Total	5.369	11			

Multiple Comparisons

LSD

Dependent Variable	(I) SL	(J) SL	Mean Difference (I-J)	Std. Error	Sig.	95% Confidence Interval	
						Lower Bound	Upper Bound
pH	Wolecho	Araticho	-.48000*	.01106	.000	-.5055	-.4545
		Zigez	-.40000*	.01106	.000	-.4255	-.3745
	Araticho	Wolecho	.48000*	.01106	.000	.4545	.5055
		Zigez	.08000*	.01106	.000	.0545	.1055
	Zigez	Welecho	.40000*	.01106	.000	.3745	.4255
		Araticho	-.08000*	.01106	.000	-.1055	-.0545
EC	Welecho	Araticho	-112.66667*	.74759	.000	-114.3906	-110.9427
		Zigez	-98.90000*	.74759	.000	-100.6239	-97.1761
	Araticho	Wolecho	112.66667*	.74759	.000	110.9427	114.3906
		Zigez	13.76667*	.74759	.000	12.0427	15.4906
	Zigez	Wolecho	98.90000*	.74759	.000	97.1761	100.6239
		Araticho	-13.76667*	.74759	.000	-15.4906	-12.0427
TUR	Wolecho	Araticho	2.16667*	.58926	.006	.8078	3.5255
		Zigez	-1.50000*	.58926	.034	-2.8588	-.1412
	Araticho	Wolecho	-2.16667*	.58926	.006	-3.5255	-.8078
		Zigez	-3.66667*	.58926	.000	-5.0255	-2.3078
	Zigez	Wolecho	1.50000*	.58926	.034	.1412	2.8588
		Araticho	3.66667*	.58926	.000	2.3078	5.0255
TSS	Wolecho	Araticho	-9.83333*	.90523	.000	-11.9208	-7.7459
		Zigez	-21.00000*	.90523	.000	-23.0875	-18.9125
	Araticho	Wolecho	9.83333*	.90523	.000	7.7459	11.9208
		Zigez	-11.16667*	.90523	.000	-13.2541	-9.0792
	Zigez	Wolecho	21.00000*	.90523	.000	18.9125	23.0875
		Araticho	11.16667*	.90523	.000	9.0792	13.2541
TDS	Wolecho	Araticho	-74.50000*	.54518	.000	-75.7572	-73.2428
		Zigez	-58.66667*	.54518	.000	-59.9239	-57.4095
	Araticho	Wolecho	74.50000*	.54518	.000	73.2428	75.7572
		Zigez	15.83333*	.54518	.000	14.5761	17.0905
	Zigez	Wolecho	58.66667*	.54518	.000	57.4095	59.9239
		Araticho	-15.83333*	.54518	.000	-17.0905	-14.5761
TA	Wolecho	Araticho	-319.66667*	13.78002	.000	-351.4434	-287.8899
		Zigez	-219.66667*	13.78002	.000	-251.4434	-187.8899
	Araticho	Wolecho	319.66667*	13.78002	.000	287.8899	351.4434
		Zigez	100.00000*	13.78002	.000	68.2232	131.7768
	Zigez	Wolecho	219.66667*	13.78002	.000	187.8899	251.4434
		Araticho	-100.00000*	13.78002	.000	-131.7768	-68.2232
TH	Wolecho	Araticho	-408.66667*	11.85796	.000	-436.0112	-381.3222
		Zigez	-308.66667*	11.85796	.000	-336.0112	-281.3222
	Araticho	Wolecho	408.66667*	11.85796	.000	381.3222	436.0112

		Zigez	100.00000*	11.85796	.000	72.6555	127.3445
	Zigez	Wolecho	308.66667*	11.85796	.000	281.3222	336.0112
		Araticho	-100.00000*	11.85796	.000	-127.3445	-72.6555
Temp	Wolecho	Araticho	-.20000	.11785	.128	-.4718	.0718
		Zigez	.00000	.11785	1.000	-.2718	.2718
	Araticho	Wolecho	.20000	.11785	.128	-.0718	.4718
		Zigez	.20000	.11785	.128	-.0718	.4718
	Zigez	Wolecho	.00000	.11785	1.000	-.2718	.2718
		Araticho	-.20000	.11785	.128	-.4718	.0718
Cl	Wolecho	Araticho	-61.10000*	2.93343	.000	-67.8645	-54.3355
		Zigez	-41.10000*	2.93343	.000	-47.8645	-34.3355
	Araticho	Wolecho	61.10000*	2.93343	.000	54.3355	67.8645
		Zigez	20.00000*	2.93343	.000	13.2355	26.7645
	Zigez	Wolecho	41.10000*	2.93343	.000	34.3355	47.8645
		Araticho	-20.00000*	2.93343	.000	-26.7645	-13.2355
Fe	Wolecho	Araticho	-1.10000*	.30641	.007	-1.8066	-.3934
		Zigez	-1.10000*	.30641	.007	-1.8066	-.3934
	Araticho	Wolecho	1.10000*	.30641	.007	.3934	1.8066
		Zigez	.00000	.30641	1.000	-.7066	.7066
	Zigez	Wolecho	1.10000*	.30641	.007	.3934	1.8066
		Araticho	.00000	.30641	1.000	-.7066	.7066

*. The mean difference is significant at the 0.05 level.

	pH	EC	TUR	TSS	TDS	TA	TH	Temp	Cl	Fe
Pearson Correlation	1	.932**	-.004	.880**	.922**	.766**	.781**	.422	.848**	.899**
Sig. (2-tailed)		.000	.990	.000	.000	.004	.003	.172	.000	.000
N	12	12	12	12	12	12	12	12	12	12
Pearson Correlation	.932**	1	-.089	.752**	.996**	.927**	.944**	.388	.958**	.846**
Sig. (2-tailed)	.000		.784	.005	.000	.000	.000	.213	.000	.001
N	12	12	12	12	12	12	12	12	12	12
Pearson Correlation	-.004	-.089	1	.433	-.168	-.307	-.259	-.159	-.284	.219
Sig. (2-tailed)	.990	.784		.160	.601	.332	.417	.622	.371	.493
N	12	12	12	12	12	12	12	12	12	12
Pearson Correlation	.880**	.752**	.433	1	.703*	.469	.511	.197	.567	.837**
Sig. (2-tailed)	.000	.005	.160		.011	.124	.090	.539	.055	.001
N	12	12	12	12	12	12	12	12	12	12
Pearson Correlation	.922**	.996**	-.168	.703*	1	.949**	.959**	.428	.976**	.829**
Sig. (2-tailed)	.000	.000	.601	.011		.000	.000	.165	.000	.001
N	12	12	12	12	12	12	12	12	12	12
Pearson Correlation	.766**	.927**	-.307	.469	.949**	1	.993**	.500	.984**	.719**
Sig. (2-tailed)	.004	.000	.332	.124	.000		.000	.098	.000	.008
N	12	12	12	12	12	12	12	12	12	12
Pearson Correlation	.781**	.944**	-.259	.511	.959**	.993**	1	.454	.984**	.731**
Sig. (2-tailed)	.003	.000	.417	.090	.000	.000		.138	.000	.007
N	12	12	12	12	12	12	12	12	12	12
Pearson Correlation	.422	.388	-.159	.197	.428	.500	.454	1	.546	.589*
Sig. (2-tailed)	.172	.213	.622	.539	.165	.098	.138		.066	.044
N	12	12	12	12	12	12	12	12	12	12
Pearson Correlation	.848**	.958**	-.284	.567	.976**	.984**	.984**	.546	1	.782**
Sig. (2-tailed)	.000	.000	.371	.055	.000	.000	.000	.066		.003
N	12	12	12	12	12	12	12	12	12	12
Pearson Correlation	.899**	.846**	.219	.837**	.829**	.719**	.731**	.589*	.782**	1
Sig. (2-tailed)	.000	.001	.493	.001	.001	.008	.007	.044	.003	
N	12	12	12	12	12	12	12	12	12	12
Pearson Correlation	.750**	.624*	.616*	.942**	.568	.363	.407	.319	.460	.825**

Sig. (2-tailed)	.005	.030	.033	.000	.054	.245	.190	.312	.133	.001
N	12	12	12	12	12	12	12	12	12	12